

Leveraging neonatal Fc receptor (FcRn) to enhance antibody transport across the blood brain barrier

Received: 26 February 2024

Accepted: 23 April 2025

Published online: 03 May 2025



Julien Lafrance-Vanasse^{1,8}, Shraddha S. Sadekar^{2,8}, Yanli Yang^{3,8}, Daniela Bumbaca Yadav², William J. Meilandt⁴, Monica K. Wetzel-Smith⁴, Hao Cai², Susan R. Crowell², Van Nguyen⁵, Vivian Lee³, Ben Chih⁶, Mandy Kwong⁶, Pamela Chan⁶, Sara Santagostino⁷, Donna Lee⁷, Shan Chung⁵, Greg A. Lazar³, James A. Ernst¹ & Jasvinder K. Atwal⁴✉

The blood-brain barrier (BBB) restricts efficient penetration of systemically delivered therapeutic antibodies into the brain, limiting the development of this class of drugs to treat neurodegenerative diseases. Here we demonstrate that the neonatal Fc receptor (FcRn), which is highly expressed at the BBB, can be used to facilitate IgG transport to the brain. Engineering of the antibody Fc region to promote binding to FcRn at neutral pH enhances antibody transcytosis in a cellular model. In vivo, these modifications improve brain penetration, as well as brain target engagement and activity, of systemically administered antibodies in both mice and non-human primates. This engineering approach can be broadly implemented to enhance central nervous system (CNS) exposure of antibody- and Fc-based drugs, improving the clinical potential of biotherapeutics for the treatment of human brain diseases.

Antibody penetration across the blood-brain barrier (BBB) is a highly restrictive process. Various methods to increase uptake of therapeutic antibodies have been explored. One widely investigated approach exploits receptor mediated transcytosis (RMT) target proteins that are highly expressed on brain endothelial cells, such as transferrin receptor (TfR)^{1–3}. RMT target binding has been engineered into IgGs through various bispecific antibody formats, including via two distinct Fabs in classic IgG format⁴, C-terminal Fab fusion⁵, and a de novo binding site engineered in the Fc region⁶. While all approaches have shown success in pre-clinical models^{6,7}, they generally also bear some limitations. For example, targeting TfR directly introduces safety liabilities due to its broad expression. In mice, acute clinical signs and infusion reactions have been observed following dosing with anti-TfR antibodies, attributed to antibody-mediated targeting of immature reticulocytes^{8,9}.

While these risks can be mitigated by antibody effector-attenuation^{8,10} or antibody formats that result in steric hindrance of Fc-gamma receptor activation⁹, such modifications may limit therapeutic application as effector function plays a critical role in the mechanism of action of some antibodies. Furthermore these complex bispecific formats are more challenging and resource intensive to produce compared to traditional IgG's. Nonetheless, the recent approval in Japan of an anti-TfR-iduronate-2-sulfatase fusion (pabinafusp alfa) for the treatment of Hunter Syndrome highlights the potential for BBB-crossing therapeutics^{11,12}. A handful of other TfR-based brain targeting therapeutics are in clinical trials (clinicaltrials.gov/ct2/show/NCT04251026; clinicaltrials.gov/ct2/show/NCT04639050; <https://clinicaltrials.gov/ct2/show/NCT05450549>). These studies will shed light on the translation of these approaches to humans. Meanwhile,

¹Department of Protein Chemistry, Genentech, Inc., South San Francisco, CA 94080, USA. ²Department of Translational Pharmacokinetics and Pharmacodynamics, Genentech, Inc., South San Francisco, CA 94080, USA. ³Department of Antibody Engineering, Genentech, Inc., South San Francisco, CA 94080, USA. ⁴Department of Neuroscience, Genentech, Inc., South San Francisco, CA 94080, USA. ⁵Department of Bioanalytical Science, Genentech, Inc., South San Francisco, CA 94080, USA. ⁶Department of Biochemical and Cellular Pharmacology, Genentech, Inc., South San Francisco, CA 94080, USA. ⁷Department of Translational Safety, Genentech, Inc., South San Francisco, CA 94080, USA. ⁸These authors contributed equally: Julien Lafrance-Vanasse, Shraddha S. Sadekar, Yanli Yang. ✉ e-mail: atwal.jasvinder@gene.com

strategies to improve brain uptake of biologics using other RMT targets continue to be explored^{15–17}.

Relatively little is understood about the intrinsic mechanism of antibody transport across the BBB. Of the known Fc receptors, neonatal Fc receptor (FcRn) is expressed abundantly at the BBB, as well as other tissues^{18,19}. FcRn plays an important role in endosomal recycling of circulating IgG and albumin, protecting them from lysosomal degradation and thereby prolonging their serum half-life^{20,21}. FcRn has also been shown to mediate cellular transcytosis. For example, during development, FcRn facilitates the transport of IgG molecules across the placental barrier²², and in some mammals the transport of IgG from milk across gut epithelial cells²³. FcRn in brain endothelial cells has been implicated as having either no effect on IgG transport across the BBB²⁴, or in facilitating the export of IgG molecules out of the brain²⁵.

IgG binding to FcRn is regulated by pH, with binding being below detectable levels at or above neutral pH, and of moderate affinity at mildly acidic pH, such as in endosomes²⁶. The selective binding to FcRn in acidic endosomes allows pinocytosed antibodies to be salvaged from lysosomal degradation, and thereby recycled. This, together with the high molecular weight of IgG's (~150 kDa) being above kidney filtration threshold, enables their long half-life in serum²⁷. Antibody engineering efforts have capitalized on this recycling mechanism to enhance pharmacokinetic properties. Numerous studies have demonstrated that Fc variants with enhanced FcRn binding at acidic pH result in extended half-life (~2–4 fold) in vivo, including in humans^{28–36}. In addition, Fc variants have been identified that improve FcRn affinity at both neutral and acidic pH^{28–30,33,37}, with the goal of promoting antibody/antigen complex uptake into endosomes, leading to antigen clearance. However, this approach can result in enhanced antibody clearance^{37–40}. The impact of Fc engineering on cellular and tissue transcytosis has not been fully explored. In polarized cells, rather than recycling to the cell surface, some endosomes transcytose their contents to the opposite side of the cell where IgG is released upon exposure to neutral pH. This pH-dependent process rescues IgG from intracellular degradation and secures delivery of intact antibodies across the cell. The high expression of FcRn on CNS endothelium¹⁸ suggests it may play an important role in transcytosis at the BBB.

We hypothesize that an antibody with optimal binding to FcRn could achieve enhanced transport across the BBB and into the brain. Here we use Fc variants with enhanced FcRn binding at neutral pH (pH 7.4) to promote IgG flux through the FcRn-regulated transcytosis pathway. Using a combination of biochemical assays, cellular models,

and in vivo studies in both mice and non-human primates, we demonstrate that improved binding to FcRn at neutral pH improves both antibody transcytosis and brain penetration. Engineering of IgG in this way can be widely used to improve BBB transport of therapeutic biologics for the CNS.

Results

Fc engineered human IgG1 with increased neutral pH FcRn affinity improved brain uptake in wild-type mice

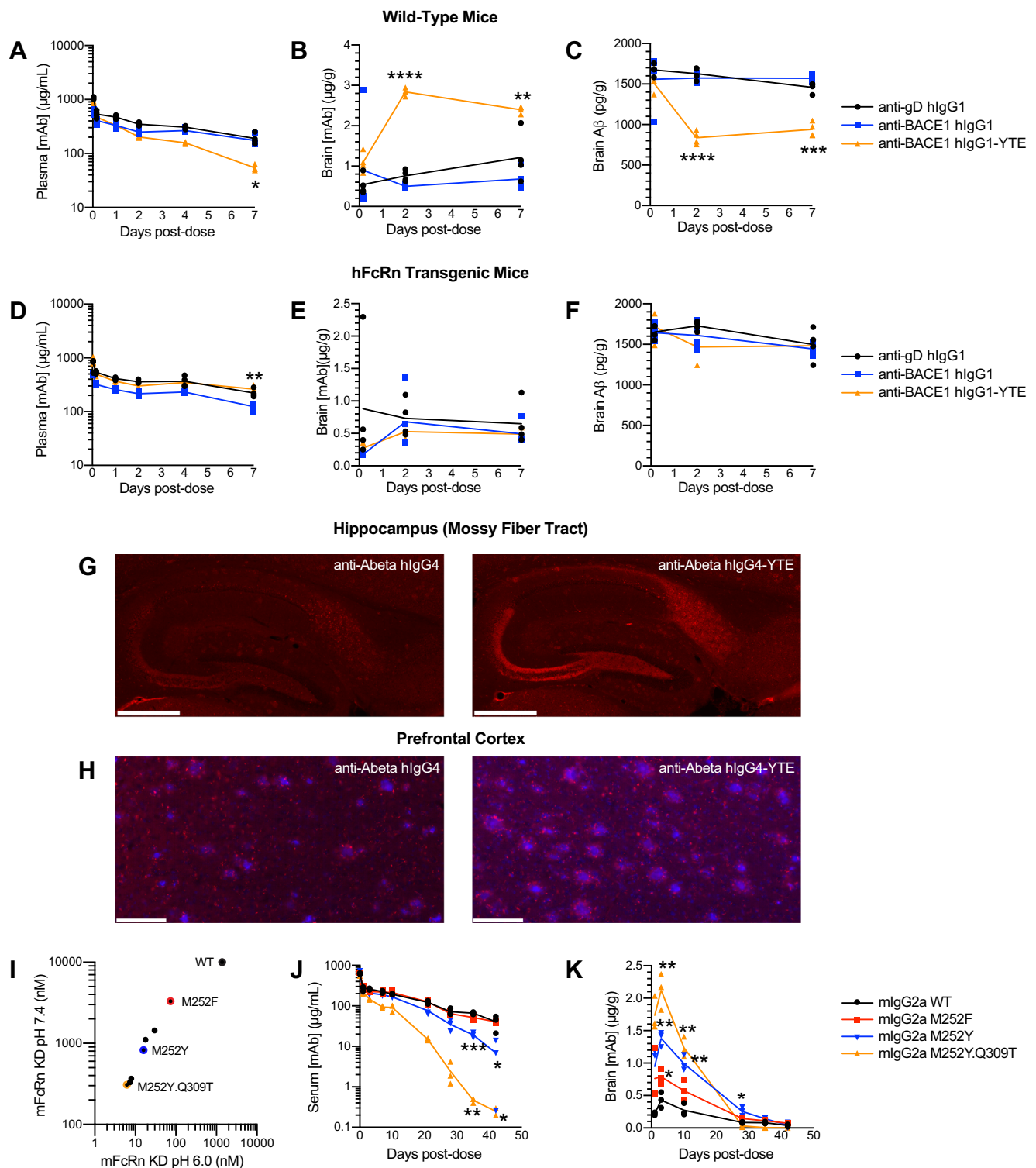
FcRn is highly expressed on CNS endothelium¹⁸. Transcriptional profiling of FACS-purified endothelial cells⁴¹ suggests some enrichment of FcRn in brain endothelial cells relative to peripheral vasculature in adult mice (Suppl. Fig. 1). We tested whether brain uptake in mice can be improved by antibodies engineered to have enhanced FcRn affinity at neutral pH. While several Fc modifications that improve binding to human FcRn (hFcRn) at pH 6.0 and/or pH 7.4 have been described, our experiment required Fc modifications that improve binding to mouse FcRn (mFcRn). We introduced a previously reported Fc modification, M252Y/S254T/T256E (YTE)²⁹, into a function-blocking anti-BACE1 hIgG1 antibody, and measured its affinity to both mFcRn and hFcRn at pH 6.0 and pH 7.4 by surface plasmon resonance (SPR) analysis. The YTE modification increased the affinity of hIgG1 binding to hFcRn at pH 6.0 by ~10-fold, whereas binding at pH 7.4 was undetectable with either a wild-type (WT) Fc or the YTE variant (Table 1). In contrast, the YTE modification improved binding to mFcRn by 16-fold at pH 6.0 and by 8-fold at pH 7.4 (Table 1), providing a tool variant to test our hypothesis. These binding results are consistent with previous reports on the impact of the YTE modification on hFcRn binding²⁹, as well as with the observation that hIgG1 binds more tightly to mFcRn as compared to hFcRn²². We dosed wild-type C57BL/6 mice with a single intravenous (IV) administration (50 mg/kg) of a control anti-gD hIgG1 antibody, anti-BACE1 hIgG1, or anti-BACE1 hIgG1-YTE to assess antibody pharmacokinetics (PK) and pharmacodynamics (PD) in vivo. Anti-BACE1 hIgG1-YTE cleared faster from systemic circulation than either antibody on WT Fc (Fig. 1A). Nonetheless, we observed improved brain antibody penetration with the YTE antibody relative to anti-BACE1 hIgG1 or anti-gD hIgG1 (Fig. 1B). Relative to anti-BACE1 hIgG1, the YTE variant increased brain concentrations by ~3-fold in terms of the maximum concentration achieved (C_{max}) and by ~4-fold in terms of the exposure (area under the curve, $AUC_{0-7 \text{ days}}$) in wild-type mice (Table 1). Consistent with the improved brain exposure, anti-BACE1 hIgG1-YTE reduced brain Amyloid β ($A\beta$)₁₋₄₀ levels (Fig. 1C),

Table 1 | Affinity (K_D), PK, and PD parameters of antibodies dosed in mouse models

Study	Fc Variant	Affinity (KD) at pH6.0 (nM)	Affinity (KD) at pH7.4 (nM)	Serum C_{max} ^a	Serum AUC ^a	Brain C_{max} ^a	Brain AUC ^a	Brain:Serum Ratio %
WT mice hIgG1 (KD to mFcRn)	anti-BACE1 WT	238	6940	1.0	1.0	1.0	1.0	0.23
	anti-BACE1 YTE	14.8	836	1.4	0.7	3.2	4.0	1.23
	anti-gD WT	ND	ND	1.8	1.3	1.4	1.5	0.26
hFcRn mice hIgG1 (KD to hFcRn)	anti-BACE1 WT	1012	>10000	1.0	1.0	1.0	1.0	0.25
	anti-BACE1 YTE	105	>10000	1.8	1.6	0.8	0.9	0.14
	anti-gD WT	ND	ND	1.6	1.6	1.3	1.3	0.20
WT mice mIgG2a (KD to mFcRn)	WT	1380	>10000	1.0	1.0	1.0	1.0	0.12
	M252F	74	3320	1.0	1.0	1.8	1.9	0.23
	M252Y	16	826	1.0	0.6	3.2	3.0	0.58
	M252Y.Q309T	6.2	308	1.0	0.3	4.9	3.4	1.26
hFcRn mice hIgG1 (KD to hFcRn)	anti-BACE1 WT	1012	>10000	1.0	1.0	1.0	1.0	0.04
	anti-BACE1 YY	13	981	1.5	0.5	2.0	1.5	0.12
	anti-BACE1 YQAY	6.9	234	1.1	0.7	5.2	4.3	0.27

Affinities (K_D) to mouse and human FcRn measured at pH 6.0 and 7.4 by SPR. Also reported are the calculated fold changes in IgG C_{max} and $AUC_{(0-7d)}$ relative to WT Fc for serum and brain. The Brain:Serum Ratio % reports the percentage of antibody measured in the brain relative to antibody measured in serum.

^a Values relative to WT, ND not done



demonstrating that the antibody was able to effectively penetrate into the brain parenchyma and reach its target in neurons. In contrast, brain Aβ₁₋₄₀ concentrations in mice dosed with anti-gD hlgG1 (control) and anti-BACE1 hlgG1 antibodies were similar and unchanged following dosing, indicating that anti-BACE1 hlgG1 with WT Fc did not reach sufficient brain concentrations to block its target. We also tested these same antibodies in hFcRn transgenic mice which express hFcRn but lack mFcRn (Tg32 *FCGRT*^{+/+} *Fcgrt*^{-/-}). In these mice, anti-BACE1 hlgG1-YTE demonstrated improved serum exposure compared to anti-BACE1-hlgG1 (Fig. 1D), consistent with previous reports. However, there was no effect on brain antibody uptake or reduction in brain

Aβ₁₋₄₀ levels (Fig. 1E, F). As the YTE variant only improves binding to hFcRn at pH 6.0 and not pH 7.4, these results suggest that higher binding affinity for FcRn at neutral pH, and not exclusively pH 6.0, enables increased transport into the brain.

Fc engineering of anti-Aβ hlgG4 improved brain uptake and target engagement in PS2APP transgenic mice

To further explore the utility of the YTE Fc modification approach, we tested whether improved brain uptake and target engagement could be achieved using an Aβ-targeting antibody in PS2APP transgenic mice, a model for Alzheimer's disease. PS2APP mice accumulate oligomeric

Fig. 1 | Antibodies with improved mFcRn affinity at neutral pH enhance brain penetration and target engagement in wild-type mice. **A–F** A single dose (50 mg/kg) of control (anti-gD), anti-BACE1, or anti-BACE1-YTE hlgG1 antibodies was delivered by IV injection to wild-type (C57BL/6J) (**A–C**) or hFcRn transgenic (Tg32) mice (**D–F**). Plasma antibody concentrations (**A, D**), brain antibody concentrations (**B, E**) and brain A β concentrations (**C, F**) were monitored for 7 days following dosing. In wild-type mice, anti-BACE1 YTE shows faster clearance (**A**), improved brain uptake (**B**) and improved pharmacodynamic activity (**C**) as compared to WT anti-BACE1. In hFcRn mice, improved serum exposure was noted for anti-BACE1 YTE over WT (**D**), while no differences in brain uptake or activity are seen (**E, F**). $n = 4$ biologically independent animals per group per time point. (**G, H**) A single IV injection (20 mg/kg) of anti-A β hlgG4 or anti-A β hlgG4-YTE was administered to PS2APP transgenic mice. 5 days later, animals were euthanized and brains harvested and assessed for target engagement (**G, H**). Antibody binding to A β in the

mossy fiber hippocampal tract (**G**) and to peri-plaque associated halos in the prefrontal cortex (**H**) was visualized by immunostaining with anti-hlgG-Alexa594 antibody (red). Plaques are labeled with methoxy-XO4 (blue). Scale bar: 500 μ m (**G**), 200 μ m (**H**). $n = 4$ biologically independent animals per group. **I–K** Non-binding antibodies bearing Fc mutations were administered to wild-type (SCID) mice by single dose IV injection (40 mg/kg). **I** Affinities (K_D) of mlgG2a variants to mFcRn at pH 6.0 and pH 7.4 as measured by SPR. Serum antibody concentration (**J**) and brain antibody concentration (**K**) were monitored for 42 days following dosing. $n = 3$ biologically independent animals per group per time point. mFcRn variants M252Y and M252Y.Q309T show faster clearance, while all variants show enhanced brain uptake through 10 days post-dose. (Statistical significance between Fc variant treated groups and respective WT treated group was evaluated over time by 2-way ANOVA or mixed effect analysis with Tukey or Dunnett's multiple comparisons test using Graphpad Prism 9.5.1; * $p < 0.05$, ** $p < 0.01$, *** $p < 0.001$, **** $p < 0.0001$).

and fibrillar amyloid deposits in the brain, including amyloid plaques⁴². We have previously shown that administration of an oligomer-preferring anti-A β antibody in these mice leads to specific antibody binding along the periphery of amyloid plaques, and along the mossy fiber hippocampal tract, two regions which bear high concentrations of A β oligomers, as demonstrated by immunostaining with an oligomeric A β antibody⁴³. We engineered the YTE modification into this anti-A β molecule on an hlgG4 isotype. Transgenic PS2APP mice received a single IV dose of either anti-A β hlgG4 or anti-A β hlgG4-YTE (20 mg/kg). Five days later, plasma was collected to determine peripheral antibody exposure, and brains were harvested and sub-dissected; one hemibrain was prepared for immunohistochemistry, and the cerebellum was used to measure brain antibody uptake.

Consistent with the anti-BACE1 hlgG1-YTE results, anti-A β hlgG4-YTE trended toward lower systemic exposure than anti-A β hlgG4 (71 ± 5 versus 127 ± 46 μ g/mL, $p = 0.1$, unpaired t -test), yet demonstrated ~3-fold higher brain concentrations at 5 days post dose (0.62 ± 0.13 versus 0.20 ± 0.12 μ g/mL, $p < 0.005$, unpaired t -test). To assess antibody partitioning to the brain more directly, these numbers can be converted to the percentage brain:serum ratio (i.e. the percentage of antibody measured in the brain relative to antibody measured in serum). At 5 days post dose, the percentage brain:plasma ratio for anti-A β hlgG4 was 0.16%, compared to 0.87% for anti-A β hlgG4-YTE, indicating improved brain partitioning with Fc modification. In vivo target engagement was assessed using immunohistochemistry (IHC) to visualize antibody binding in the mossy fiber hippocampal tract (Fig. 1G) or surrounding amyloid plaques in the prefrontal cortex (Fig. 1H). Qualitatively, both regions showed more robust staining following dosing with anti-A β hlgG4-YTE compared to anti-A β hlgG4. Across the brain, the overall pattern of binding appeared similar for both anti-A β hlgG4 and anti-A β hlgG4-YTE, with a greater intensity of staining detected for the YTE variant (Suppl. Fig. 2). No binding was seen with a control anti-gD hlgG4 antibody (Suppl. Fig. 2). Quantitative analysis was performed on the mossy fiber binding and showed an increase in integrated density for anti-A β hlgG4-YTE over anti-A β hlgG4 (1.03 ± 0.11 E5 versus 4.8 ± 2.7 E4, $p < 0.01$ unpaired t -test).

Increased brain uptake of mouse IgG2a Fc variants in mice

To explore whether the human IgG results could be extended to antibodies with a murine backbone, we set out to identify antibody Fc region modifications in mouse isotype mlgG2a that improve affinity to mFcRn at pH 7.4. Based on the published FcRn-Fc structure [PDB 1IA⁴⁴], we identified four regions of the Fc in close contact with FcRn: 248-259; 284-290; 306-317; 426-438 (EU numbering). An NNK walk phage display library was then created, where each residue in these regions was mutated to all other amino acids, except histidines which were left unaltered. Only the Fc region was displayed at the surface of the phage. After 3 rounds of panning against mFcRn, we analyzed the samples by Next Generation Sequencing (NGS) and looked for substituted positions with significantly enriched sequence read counts,

compared to the original library (Suppl. Fig. 3). Residues with the greatest and most consistent enrichment included Met252, when substituted with an aromatic residue (Phe or Tyr), and Gln309 when substituted to either Ser or Thr.

We then incorporated Fc substitutions at Met252 alone or in combination with Gln309 into full-length mlgG2a antibodies with a non-binding Fab and measured their affinity to mFcRn by SPR at both pH 6.0 and 7.4 (Fig. 1I, Suppl. Table 1). The double variants had a higher affinity to mFcRn at pH 7.4 than any of the single mutants. Interestingly, for all variants, the increase in mFcRn affinity at pH 7.4 was associated with an increase in affinity at pH 6.0. With this panel of variants, a wide range of affinities was covered.

Engineering anti-TfR antibodies to cross the BBB requires optimization of TfR affinity^{4,45}. We hypothesized that this would also be the case for FcRn receptor-mediated transcytosis and selected 3 variants with different affinities to FcRn at pH 7.4 to test in vivo: M252F (3320 nM), M252Y (826 nM), and M252Y.Q309T (308 nM). We injected these variants into wild-type SCID mice at a dose of 40 mg/kg (IV), and euthanized animals at several time points over a period of 42 days to measure the antibody concentrations in both serum and brain (Fig. 1J, K). Systemic antibody clearance was increased for the M252Y and M252Y.Q309T variants, with an apparent trend between tighter mFcRn affinity at pH 7.4 and greater serum antibody clearance (Fig. 1J). M252F mlgG2a, which had the smallest change in affinity to mFcRn of all the variants, cleared at the same rate as the WT antibody in serum. Improved antibody uptake in the brain was observed for all three variants (Fig. 1K), and was reflected by increases in both C_{max} and the AUC₀₋₇ values (Table 1). Brain antibody uptake trended to increase directly with antibody affinity to mFcRn at pH 7.4. M252Y.Q309T mlgG2a crossed the BBB most efficiently, with C_{max} 4.9-fold higher and AUC 3.4-fold higher than WT mlgG2a. Re-plotting of serum and brain antibody concentrations together on a logarithmic scale (Suppl. Fig. 4) shows that brain and serum antibody clearance over time approximately parallels each other for the different variants, suggesting serum concentration is the primary driving force of antibody concentration in the brain.

Engineered human IgG1 Fc variants improve in vitro transcytosis

Our results demonstrate that Fc modifications that increase IgG binding to mFcRn at pH 7.4 enhance antibody uptake into the mouse brain. In order to translate these findings to a human therapeutic approach, we next engineered Fc variants that increase affinity of hlgG1 to hFcRn at pH 7.4. Substitutions at several Fc residues in hlgG1 have previously been reported to improve binding to hFcRn^{34,37,46}. We explored these known sites combinatorially to identify candidate variants (Fig. 2A). We generated single, double, triple and quadruple Fc substitutions (Suppl. Table 2) on anti-BACE1 hlgG1, including previously described combinations (YY, YEY, YPY, and YQAY)³⁷. Variant and WT antibodies were expressed, purified, and screened for hFcRn binding and in vitro transcytosis.

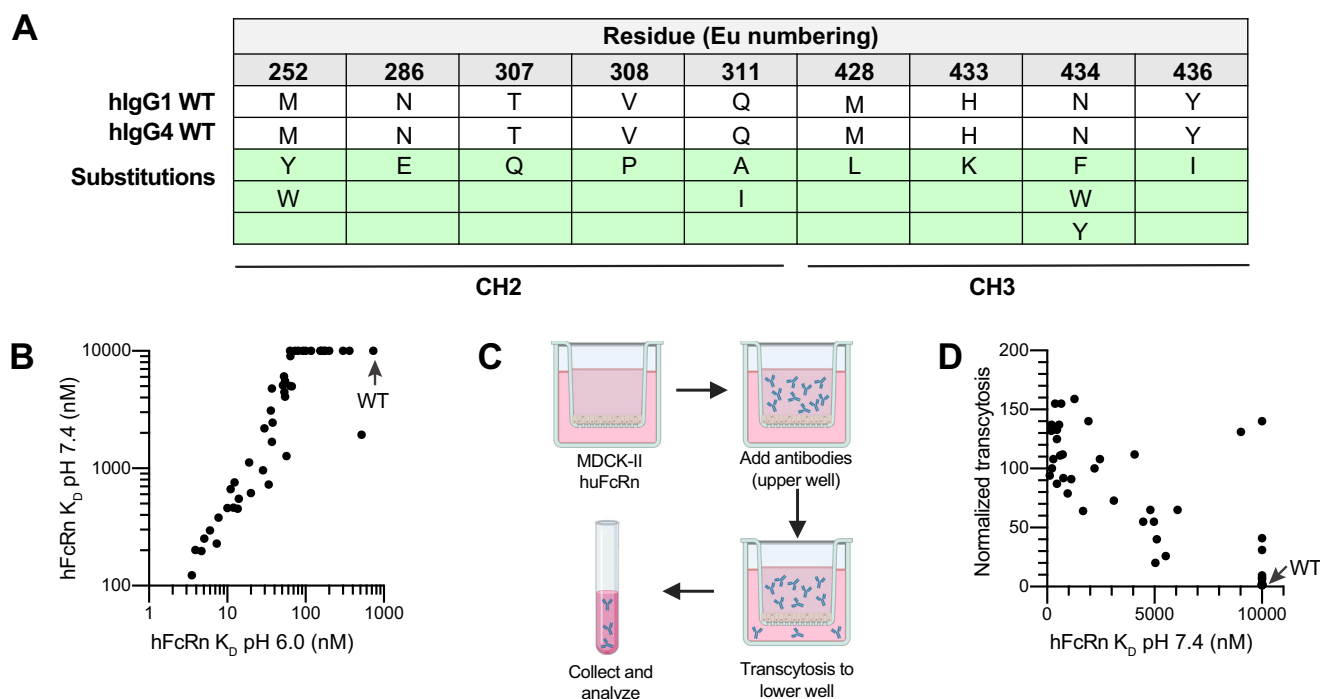


Fig. 2 | Engineering of human IgG1 antibodies for improved FcRn affinity at neutral pH leads to increased transcytosis in vitro. **A** Table showing the 9 residue positions in the CH2 and CH3 regions that were substituted, either individually or as a combination of 2, 3 or 4 positions. **B** Affinities (K_D) of the engineered variants to hFcRn at pH 6.0 and 7.4, as measured by SPR. **C** Schematic of the transcytosis assay: MDCK-II cells expressing hFcRn were cultured in a transwell plate. After

addition of antibodies in the upper well, the plate was incubated for 24 h to allow transcytosis to the lower well, where antibodies are collected and their concentrations measured. **D** Transcytosis of all engineered Fc variants, normalized to WT hIgG1 Fc, compared to hFcRn affinity at pH 7.4. Transcytosis overall trended positively with affinity. Figure 2C was created in BioRender. Lafrance-Vanasse, J. (2025) <https://BioRender.com/bcOteil>.

First, we measured the affinity of the variants to hFcRn by SPR at both pH 6.0 and pH 7.4. All variants improved hFcRn affinity at pH 6.0, and several improved affinity at pH 7.4 (Suppl. Table 2). Similar to our observations with mIgG2a, increased binding at pH 7.4 trended with increased binding at pH 6.0 (Fig. 2B). We next characterized a subset of the variants in a panel of assays to assess any impact on the biophysical and functional properties of the IgG. All variants had a moderately reduced T_m by differential scanning fluorimetry, suggesting a slight destabilization of the Fc (Suppl. Fig. 5A). Substitutions V308P and Q311I were generally more destabilizing than other substitutions. Protein A binding was minimally affected across the variant set (1-2 fold, Suppl. Fig. 5B), suggesting the variants should not impact downstream purification. Finally, the variation in affinity to Fc γ R's was also minimal (1-2 fold, Suppl. Fig. 5C-F), suggesting Fc γ R-mediated effector functions should be preserved.

To test the hypothesis that Fc variants with improved FcRn affinity at pH 7.4 can enhance transcytosis, we used a cell-based transcytosis assay previously developed to predict the PK properties of antibodies⁴⁷. This assay uses MDCK-II cells that stably overexpress hFcRn at high levels. Briefly, cells were grown in a transwell plate as a monolayer sheet with tight junctions, ensuring a tight seal between the upper and lower wells (Fig. 2C). Media in both wells was maintained at pH 7.4. Antibodies were added to the upper well, and after 24 h, media from the lower well was harvested to quantitate transcytosed antibody. Minimal to modest improvements in transcytosis (1.7 - 7.8-fold) were observed for most Fc modified antibodies with enhanced hFcRn affinity at pH 6.0 but unmeasurable affinity at pH 7.4 (Fig. 2D, Suppl. Table 2). In contrast, antibodies comprising double, triple, and quadruple Fc modifications with improved hFcRn binding at pH 7.4 showed markedly enhanced transcytosis, with some Fc modifications promoting transcytosis up to ~150 fold relative to WT IgG1.

Engineered human IgG1 Fc variants increased brain uptake in hFcRn transgenic mice

We selected 14 hlgG1 variants that demonstrated improved cellular transcytosis and retained favorable molecular properties to advance to in vivo brain penetration studies in hFcRn transgenic mice. Following administration of a single IV dose of 50 mg/kg, serum was sampled at 3 and 7 days post-dose to determine peripheral exposure (AUC_{0-7}). Serum exposure of all of the Fc modified antibodies was reduced relative to WT hlgG1 (Fig. 3A). As many of the antibodies tested cleared rapidly, we analyzed brains harvested 3 days post-dose to assess brain uptake. A majority of the Fc modified antibodies showed improvements in brain antibody concentration, up to ~2.5 fold relative to WT hlgG1 (Fig. 3B). A few variants showed brain concentrations less than WT hlgG1, and these antibodies also demonstrated fast clearance from serum. The percentage brain:serum ratio 3 days post dose (anticipated maximal concentration in brain) for the various antibodies is plotted against the antibody affinity for hFcRn at pH 7.4 in Fig. 3C. Consistent with previous reports⁴, WT hlgG1 shows a brain:serum ratio of ~0.1 in mice. Most of the Fc variants showed an enhanced brain:serum ratio, reaching as high as 1.5%, and the improvement in brain partitioning using this measure demonstrated a direct trend with hFcRn affinity at pH 7.4. These results demonstrate that engineering IgG1 with improved FcRn affinity at pH 7.4 promotes enhanced transcytosis and brain partitioning of antibodies.

Engineered human IgG1 Fc variants improved pharmacodynamic response in hFcRn transgenic mice

Two anti-BACE1 hIgG1 Fc variants (YY and YQAY) were selected to explore whether enhanced brain uptake translates to more BACE1 inhibition, and consequently greater reduction of brain A β ₁₋₄₀. A single IV dose of 50 mg/kg anti-BACE1 hIgG1 WT, anti-BACE1-hIgG1-YY, or anti-BACE1-hIgG1-YQAY was administered to hFCrn transgenic mice.

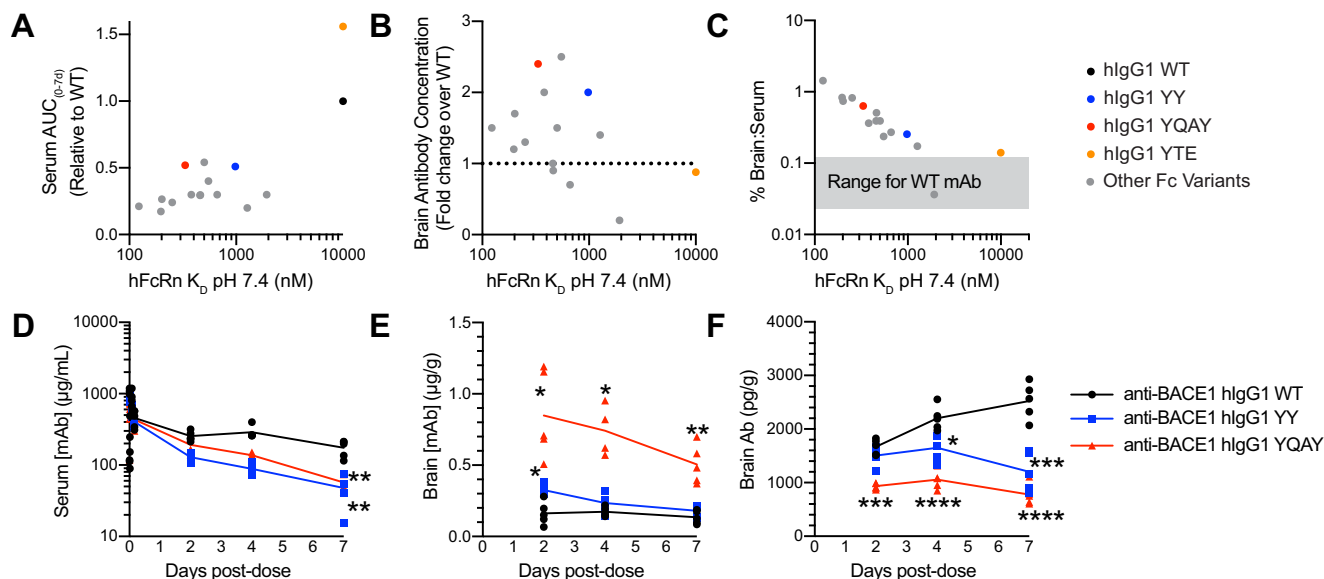


Fig. 3 | Human IgG1 antibodies with Fc engineered for improved FcRn affinity at neutral pH demonstrate increased serum clearance, enhanced brain uptake and partitioning, and improved target engagement in hFcRn mice. A–C A single IV injection (50 mg/kg) of engineered human IgG1 Fc region variants was administered to hFcRn transgenic mice. Serum antibody exposure (AUC) over 7 days (A), brain antibody concentration at day 3 (B) and % brain:serum ratio at day 3 (C) are plotted as correlations to hFcRn affinity at pH 7.4 for each variant. $n = 4$ biologically independent animals per group per time point. YTE results from Fig. 1D–F are included to represent an antibody with improved hFcRn affinity at pH 6.0 but not

7.4. (Note: YY data points are derived from data in Fig. 3D, E). **D–F** A single IV injection (50 mg/kg) of anti-BACE1 hlgG1 WT or FcRn 7.4 variants YY or YQAY was administered to hFcRn transgenic mice. The Fc variant antibodies demonstrated faster serum clearance (D), higher brain antibody concentrations (E), and reduced brain Aβ concentrations (F) over 7 days post-dose. $n = 5$ biologically independent animals per group per time point. (Statistical significance between Fc variant treated groups and respective WT treated group was evaluated over time by 2-way ANOVA or mixed effect analysis with Tukey or Dunnett's multiple comparisons test using Graphpad Prism 9.5.1; * $p < 0.05$, ** $p < 0.01$, *** $p < 0.001$, **** $p < 0.0001$).

Serum and brain samples were collected at 2, 4, and 7 days post-dose to assess antibody concentrations and brain Aβ₁₋₄₀ concentrations. Anti-BACE1-hlgG1-YY and anti-BACE1-hlgG1-YQAY showed reduced serum exposure compared to anti-BACE1-hlgG1 WT (Fig. 3D), consistent with previous results (Fig. 3A). Anti-BACE1-hlgG1-YQAY showed a sustained and statistically significant improvement in brain uptake, while anti-BACE1-hlgG1-YY trended towards enhanced brain uptake compared to anti-BACE1-hlgG1 WT (Fig. 3E, Table 1). We next assessed brain Aβ₁₋₄₀ concentrations from mice dosed with the different antibodies. Brains from mice dosed with anti-BACE1-hlgG1 WT had lower brain Aβ₁₋₄₀ at early time points, which increased by day 7 (Fig. 3F), suggesting early, transient inhibition of BACE1 activity. Consistent with having higher concentrations of antibody in brain, mice dosed with anti-BACE1-hlgG1-YQAY had lower concentrations of brain Aβ₁₋₄₀ at all time points, with the greatest difference at day 7, suggesting sustained BACE1 inhibition in the brain. Mice dosed with anti-BACE1-hlgG1-YY had intermediate concentrations of brain Aβ₁₋₄₀, suggesting improved target engagement relative to anti-BACE1-hlgG1 WT. In summary, anti-BACE1-hlgG1-YQAY robustly improved brain antibody uptake, both by C_{max} (5.2 fold) and AUC (4.3 fold), and reduced brain Aβ₁₋₄₀ levels more effectively than anti-BACE1-hlgG1 WT (Table 1). Anti-BACE1-hlgG1-YY demonstrated similar, albeit more modest, improvements in brain uptake and Aβ₁₋₄₀ reduction.

Anti-BACE1 hlgG1 Fc variants enhanced brain uptake and pharmacodynamic response in cynomolgus monkeys

To further support clinical translation, we next tested whether anti-BACE1 hlgGs engineered for increased FcRn binding at pH 7.4 increase brain uptake in non-human primates (NHP). Antibody affinities to cynomolgus monkey FcRn were generally comparable to human FcRn (Suppl. Table 3). Two separate studies were carried out, each administering a single 50 mg/kg IV dose to cynomolgus monkeys. In the first study, animals ($n = 4$) were dosed with WT anti-BACE1 hlgG1 or one of the Fc variants YYY, YQAY, or YPY, with serum samples collected

through 28 days post-dose, and cerebrospinal fluid (CSF) samples through 7 days post-dose. In the second study, animals ($n = 4$) were dosed with WT anti-BACE1 hlgG1 or Fc variant YY or YQAY. Serum and CSF samples were collected up to 7 days post-dose, and 2 animals each were euthanized at 2 and 7 days post-dose to collect brain samples to measure antibody uptake and pharmacodynamic response, as well as other tissues to measure antibody distribution. Across both studies, the Fc variant antibodies were generally well-tolerated in monkeys, with no major clinical signs, gross findings or body weight loss observed.

Analysis of the data over the first 7 days post-dose revealed that anti-BACE1 Fc variants distributed and cleared more quickly than the WT Fc antibody, with higher affinity variants clearing faster (Fig. 4A). This is consistent with our observations in mice. Over 28 days post-dose, serum antibody concentrations continued to drop (Fig. 4B). For most animals dosed with Fc variants, antibody concentrations dropped faster than expected for conventional antibody elimination, suggestive of anti-drug antibody response. At 2 days post-dose anti-BACE1 hlgG1 YY and YQAY variants demonstrated ~7.5-fold higher average brain concentrations relative to the WT antibody (Fig. 4C, Table 2). This improvement in brain uptake was maintained at day 7. The higher brain concentrations observed, despite faster plasma clearance for the Fc variants, suggests a greater distribution from plasma to CNS relative to WT. When calculated as percentage brain:serum ratio at 2 days post dose (maximal anticipated brain concentration), Fc variants showed ~0.4–0.8% antibody partitioning to the brain, as compared to only 0.01% for WT antibody (Fig. 4D), with similar improvements maintained at day 7. In the CSF, antibody concentrations of Fc variants were similar to or greater than concentrations of the WT antibody (Fig. 4E). When calculated as percentage CSF:serum ratio, all Fc variants demonstrated greater partitioning to the CSF compared to WT hlgG, in an FcRn affinity-dependent manner (Fig. 4F).

To assess target engagement, we measured the sAPPβ/α ratio in CSF and brain, a reflection of APP processing by BACE1. The anti-BACE1

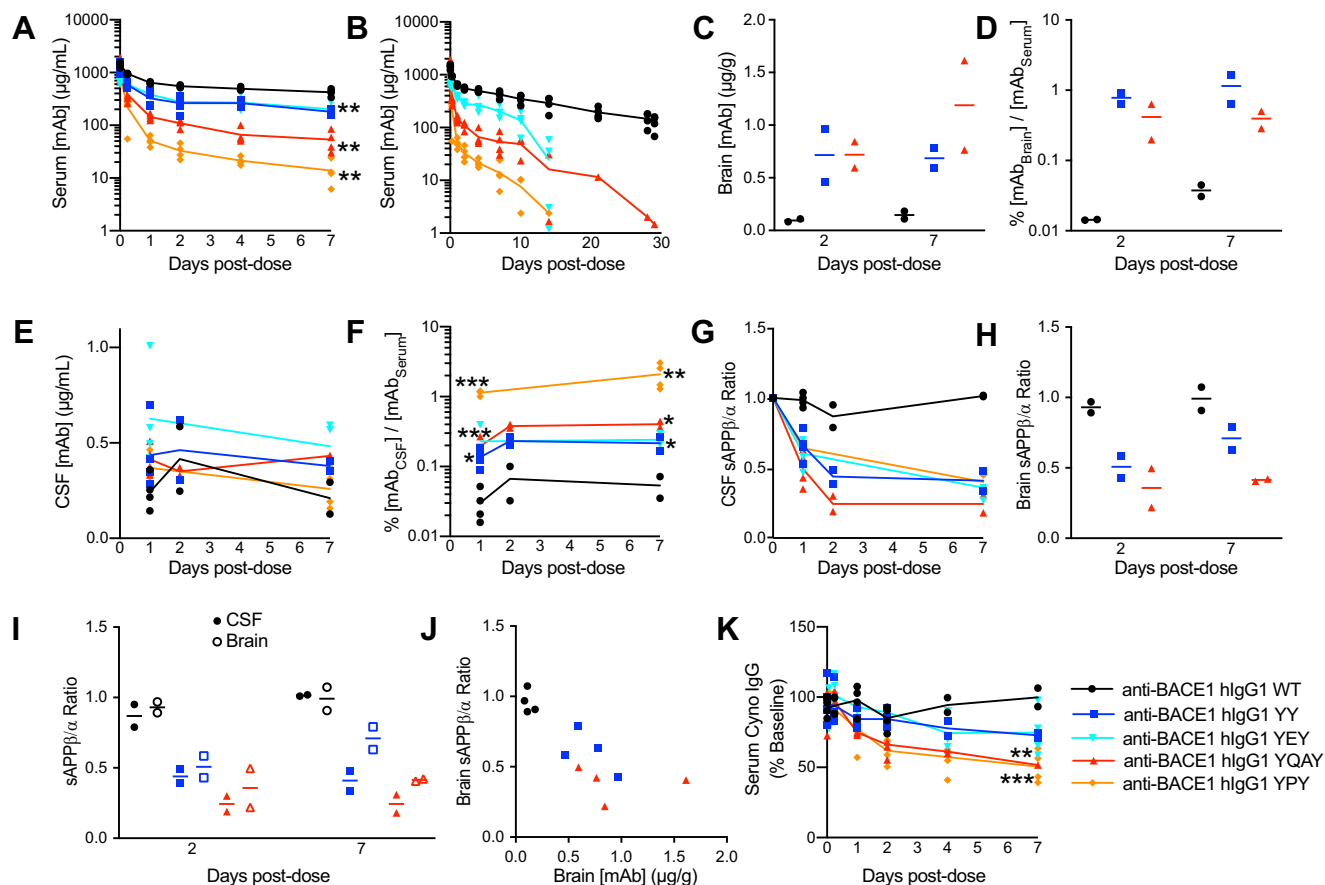


Fig. 4 | Anti-BACE1 hlgG1 variants with improved affinity to primate FcRn at neutral pH demonstrate faster serum clearance and improved brain uptake and enhanced CNS pharmacodynamic response in cynomolgus monkeys. A single dose (50 mg/kg) of anti-BACE1 hlgG1 or hlgG1 Fc variants with enhanced binding to human and cynomolgus monkey FcRn at neutral pH (YY, YQAY, YPY) was delivered by IV injection to cynomolgus monkeys (*n* = 4 per group). Fc variants show reduced serum antibody concentrations compared to WT hlgG1 over the first 7 days post-dose (A), indicative of faster clearance. Serum antibody concentrations continue to drop over 28 days post-dose (B). Brain tissue was collected from animals dosed with anti-BACE1-WT, anti-BACE1-YY or anti-BACE1-YQAY at 2 or 7 days post-dose, and average brain antibody concentrations were determined (2 animals per time point) (C). BACE1 antibodies with modified Fcs were present at higher concentrations in brain than the anti-BACE1 WT Fc antibody. The ratio of the concentration of antibody in the brain relative to the concentration of antibody in the serum (D) shows that the modified Fcs (YY, YQAY) resulted in an increase in the proportion of anti-BACE1 antibody in the brain. Mean CSF antibody concentrations

at 1, 2 or 7 days post-dose were also measured, and are reported as either absolute concentration (E) or as a ratio of the concentration in CSF relative to the concentration in the serum (F). Anti-BACE1 antibodies with modified Fcs showed a trend for greater CSF concentrations and partitioning as compared to anti-BACE1 with a WT Fc. Anti-BACE1 hlgG1 Fc variants showed a reduction in sAPPβ/α ratio in the CSF (G) and brain (H). The extent of reduction was comparable in brain (open symbols) and CSF (closed symbols) (I). sAPPβ/α ratio decreased with higher brain concentrations of the Fc variant antibodies (J). Anti-BACE1 hlgG1 Fc variants showed a decrease in circulating endogenous levels of IgG (K). The number of biologically independent animals per group is: *n* = 4 for serum measurements, except Day 7 YY *n* = 2; *n* = 4 for CSF measurements, except Day 2 YY, YQAY and Day 7 YY *n* = 2; *n* = 2 for all brain measurements. (Statistical significance between Fc variant treated groups and respective WT treated group was evaluated over time by 2-way ANOVA or mixed effect analysis with Tukey or Dunnett's multiple comparisons test using Graphpad Prism 9.5.1; **p* < 0.05, ***p* < 0.01, ****p* < 0.001, *****p* < 0.0001).

antibodies with modified Fc's significantly decreased the sAPPβ/α ratio post-dose in the CSF (Fig. 4G), and also decreased the brain sAPPβ/α ratio compared to WT anti-BACE1 hlgG1 (Fig. 4H), indicating BACE1 inhibition. Good correspondence of sAPPβ/α ratio measurements was observed between the CSF and brain compartments (Fig. 4I). There was an inverse relationship between brain sAPPβ/α ratio and brain antibody concentration (Fig. 4J), indicating that higher levels of anti-BACE1 antibody in the brain result in lower sAPPβ/α ratios and more robust PD response.

Since our Fc variant antibodies are engineered to enhance FcRn affinity, they may compete with endogenous IgGs for FcRn-mediated recycling. Serum concentrations of cynomolgus IgG were reduced in animals dosed with Fc variant antibodies as compared to animals dosed with WT, with higher FcRn affinity correlating with greater IgG reduction (Fig. 4K). The effect was reversible, with IgG levels returning to baseline as Fc variants were cleared out of plasma (Suppl. Fig. 6A). Antibody concentrations were also evaluated in other tissues. Anti-

BACE1 Fc variants showed a slight increase in kidney and liver, albeit not as significant as the brain. (Suppl. Fig. 7). Serum albumin levels were unaltered, indicating that FcRn expression levels and recycling activity are normally maintained (Suppl. Fig. 8A).

Anti-Aβ hlgG4 Fc variants enhanced brain uptake in cynomolgus monkeys

We also tested anti-Aβ hlgG4 antibodies with WT Fc, or carrying the Fc modification YY, YQAY, or YPY in cynomolgus monkeys. A single 50 mg/kg IV dose was administered to animals (*n* = 7). Serum samples were collected up to 28 days post-dose, CSF samples were collected up to 7 days post-dose, and 2 animals from each group were euthanized at 2 and 7 days post-dose to collect brain samples to measure antibody exposure and assess pharmacodynamic response. The Fc variant antibodies were well tolerated in this study.

Similar to results with the anti-BACE1 hlgG1 antibodies, the anti-Aβ hlgG4 antibodies with modified Fc regions cleared more quickly from

Table 2 | Affinity (K_D), PK, and PD parameters of antibodies dosed in cynomolgus monkeys

Study	Fc Variant	Affinity (KD) to cFcRn at pH6.0 (nM)	Affinity (KD) to cFcRn at pH7.4 (nM)	Serum C_{max}^a	Serum AUC^a	Brain mAb	Brain: Serum Ratio %	Brain PD Resp	CSF mAb.	CSF: Serum Ratio %
Cyno anti-BACE1 hlgG1	WT	253	>10000	1.0	1.0	1.0	0.01	1.0	1.0	0.03
	YY	11	376	0.9	0.5	7.4	0.42	0.5	1.9	0.14
	YEY	8.7	288	0.5	0.5	N/A	N/A	N/A	3.3	0.23
	YQAY	6.7	153	0.9	0.2	7.5	0.78	0.4	1.7	0.20
	YPY	4.4	64	0.6	0.1	N/A	N/A	N/A	2	1.14
Cyno anti-A β hlgG4	WT	253	>10000	1.0	1.0	1.0	0.03	1.0	1.0	0.14
	YY	11	536	0.7	0.6	2.7	0.14	2.2	1.3	0.30
	YEY	9	265	0.8	0.7	4.7	0.18	2.9	1.7	0.34
	YQAY	6.9	193	0.8	0.5	4.1	0.28	2.9	1.9	0.59

Affinities (K_D) to cyno FcRn (cFcRn) as measured at pH 6.0 and 7.4 by SPR. Also reported are the calculated fold changes in IgG C_{max} and AUC_{0-7d} relative to WT Fc for serum. Serum data after day 7 is excluded from analysis due to consistent impact of ADA on PK. In brain, antibody concentration fold change, brain:serum ratio %, and PD fold change are reported for Day 2. In CSF, antibody concentration fold change and CSF:serum ratio % are reported for Day 1 in the anti-BACE1 hlgG1 study, and Day 2 in anti-A β hlgG4 study. Brain PD response reports the sAPP β /a ratio (relative to WT) in the anti-BACE1 study, and A β concentrations (relative to WT) in the anti-A β study. For anti-BACE1, the following data came from Study 2: YY serum, all brain data, CSF for YY, YQAY; all other data is from Study 1.

^a values relative to WT; N/A = not applicable (no sample).

serum than WT anti-A β hlgG4 antibody (Fig. 5A, B). Fc variant anti-A β antibodies showed ~3–5 fold greater brain uptake compared to WT Fc at day 2 and maintained that enhancement at day 7 (Fig. 5C, Table 2). 0.1–0.4% of the Fc variant antibodies present in serum distributed to the brain, as compared to only 0.03–0.04% of WT (Fig. 5D). Analysis of average CSF concentrations (Fig. 5E) and percentage CSF:serum concentrations (Fig. 5F) revealed increased partitioning of Fc variant anti-A β antibodies to CSF relative to WT hlgG4.

All animals dosed with Fc variant antibodies had higher levels of brain A β ₁₋₄₂ compared to animals dosed with WT anti-A β (Fig. 5G), suggesting higher target engagement in the CNS. Brain A β ₁₋₄₂ concentration showed a trend for increase with brain antibody concentration across the different antibodies examined (Fig. 5H). This increase in brain A β ₁₋₄₂ is likely explained by prolonged half-life of soluble A β when complexed with antibody in the brain, similar to what has been reported in plasma⁴⁸. Serum concentrations of cynomolgus IgG were again reduced in animals dosed with Fc variant anti-A β antibodies as compared to animals dosed with WT (Fig. 5I), and returned to baseline as Fc variants cleared out of plasma (Suppl. Fig. 6B). Serum albumin levels were unaltered after dosing with anti-A β Fc variants, suggesting that FcRn expression levels and recycling activity were unaffected (Suppl. Fig. 8B).

To more fully explore the relationships between FcRn affinity and antibody clearance and distribution, we performed an analysis of data across hFcRn transgenic mouse and NHP in vivo studies. Figures 6A–D combine NHP data for anti-BACE1 hlgG1 (blue triangles) and anti-A β hlgG4 (red squares) antibodies, and incorporate data from hFcRn transgenic mice dosed with anti-BACE1 hlgG1 (black circles) in Fig. 6A, C. The aggregate data show clearly that FcRn affinity at pH 7.4 has a negative association with serum exposure (Fig. 6A) and concentration of endogenous IgG (Fig. 6B), and a positive association with IgG partitioning to brain (Fig. 6C) and CSF (Fig. 6D).

Discussion

Our studies demonstrate that antibodies with Fc regions engineered to increase affinity for FcRn at pH 7.4 can enhance cellular transcytosis in vitro and improve brain partitioning in vivo. Engineered variants increased brain exposure by up to 5 fold in mouse models, and up to 7 fold in cynomolgus monkeys. These improvements were consistent across antibodies with different Fabs (anti-BACE1, anti-A β , and non-binding) and different IgG subclasses (hlgG1, hlgG4, and mlgG2a), suggesting this approach should be broadly applicable for antibody-based biotherapeutics. Increased exposure corresponded with improved pharmacodynamic response in the CNS, indicating that

antibodies reached their targets and site of action within the brain parenchyma. When normalized to respective serum levels, the percentage brain:serum ratio increased with tighter FcRn affinity at neutral pH (Fig. 6C). These results support a mechanism whereby FcRn promotes receptor-mediated transcytosis and transport of antibodies across the BBB in a manner that is dependent on FcRn affinity at pH 7.4.

The FcRn receptor is highly expressed at the BBB, where it has previously been proposed to mediate IgG efflux out of the brain⁴⁹. The efflux rate of radiolabeled IgG injected directly into the brain was found to be dependent on FcRn affinity, whereby an antibody having tighter FcRn binding at pH 6.0 was transported out of the brain more rapidly than one that bound poorly to FcRn²⁵. A separate study showed that in FcRn knockout mice, partitioning of IgG in brain relative to blood following IV administration was unaltered relative to that in wild-type mice²⁴, suggesting that FcRn does not play a role in transport of IgG into the brain, at least following systemic dosing. Together, these studies led to the conclusion that FcRn either plays no role in mediating antibody flux across the BBB, or promotes efflux of IgG from the CNS. A recent publication provides an alternative hypothesis, demonstrating that Fc engineering to enhance FcRn interaction can promote uptake of antibodies across the BBB⁵⁰, consistent with our findings.

While these results may seem at odds with one another, we believe these findings can be reconciled and together provide a better understanding of the role of FcRn at the BBB. FcRn promotes both endosomal recycling and cellular transcytosis of IgG. FcRn-mediated transcytosis is initiated by fluid-phase pinocytosis of IgG on one side of a polarized cell layer. A fraction of IgG then binds in a pH-dependent manner to FcRn once localized in acidified endosomal compartments. The endosomes enter sorting tubules, some of which are directed to transcytose to the opposite side of the cell, releasing IgG upon exposure to neutral pH. This pH-dependent process rescues IgG from intracellular degradation and delivers intact antibodies across the cell (Fig. 6E). Enhanced binding of IgG to FcRn at neutral pH promotes ligand-receptor engagement at the cell surface, driving more IgG into and in turn across the cell, thereby effectively converting FcRn into an RMT target. Notably, the IgG/FcRn interaction in our engineered molecules is still relatively low affinity at pH 7.4 (hundreds of nM), thus allowing for IgG release once transcytosis is complete and the antibody is re-exposed to the extracellular milieu. Since transcytosis is a bidirectional process, enhanced transcytosis would likely be observed in both directions in a polarized cell, with net gain occurring down a concentration gradient. The observation that intracranially delivered antibodies with increased FcRn affinity are effluxed from brain (down a

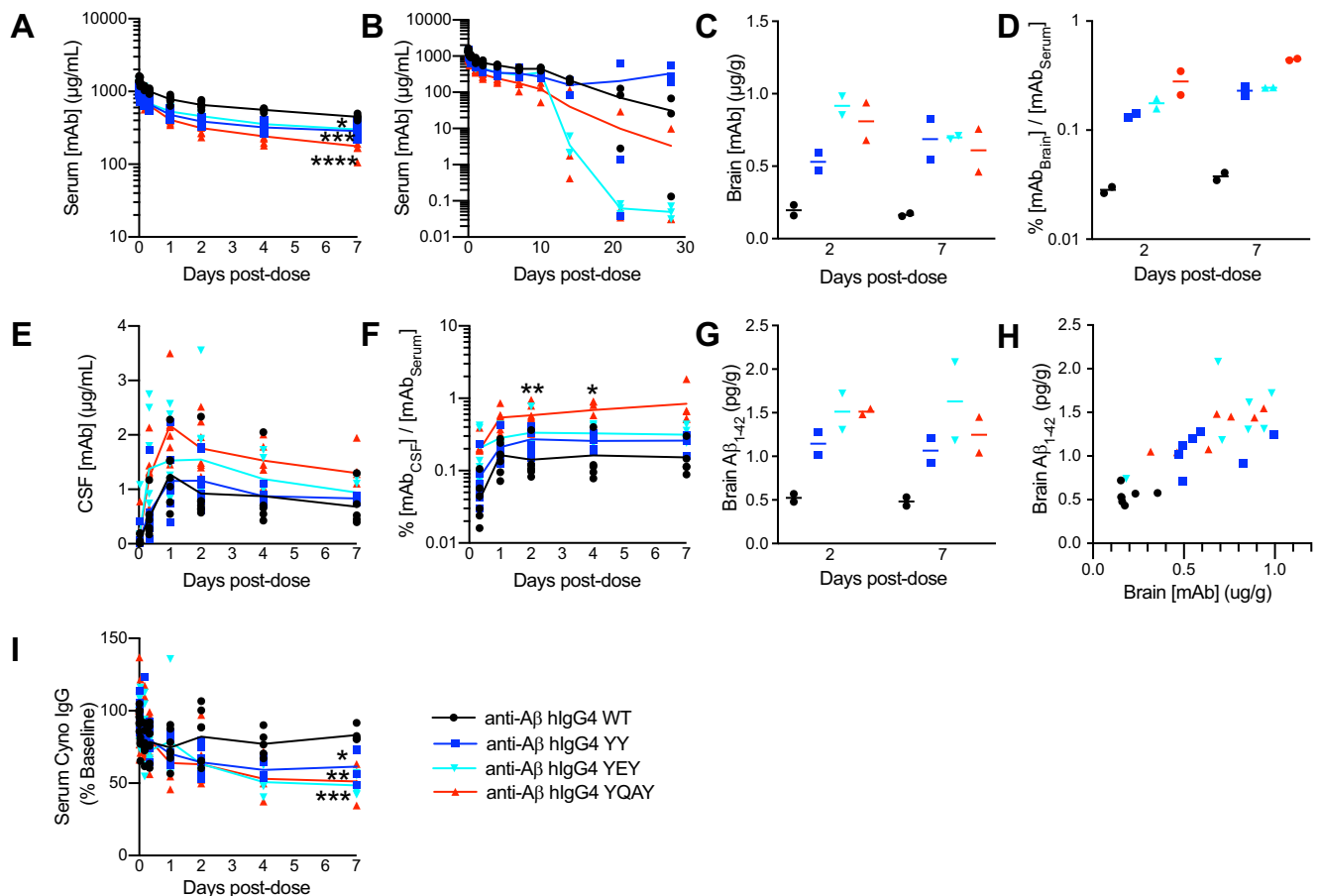


Fig. 5 | Anti-A β hlgG4 variants with improved affinity to primate FcRn at neutral pH demonstrate faster serum clearance, improved brain uptake and enhanced CNS target engagement in cynomolgus monkeys. A single dose (50 mg/kg) of anti-A β hlgG4 or hlgG4 Fc variants with enhanced binding to FcRn at neutral pH (YY, YEY, YQAY), was delivered by intravenous injection to cynomolgus monkeys ($n = 4$ per group). Two animals each were euthanized at either 2 or 7 days post-dose to determine antibody exposure and target engagement in the brain and CSF. Fc variants show reduced serum antibody concentrations compared to WT hlgG1 over the first 7 days post-dose (A). Serum antibodies concentrations continue to drop over 28 days post-dose (B). Brain tissues were collected and homogenized to determine average brain antibody concentrations. C Anti-A β antibodies with modified Fcs (YY, YEY, YQAY variants) were present at higher concentrations in brain than the anti-A β WT Fc antibody. Mean CSF antibody concentrations at 1, 2 or 7 days post-dose were also measured (E). Anti-A β antibodies with modified Fcs (YY, YEY and YQAY) showed a trend for higher CSF concentrations compared to anti-A β with a wild-type Fc. The ratio of the concentration of anti-A β antibody in the brain (D) and CSF (F) to the concentration of anti-A β antibody in the serum shows that the modified Fcs (YY, YEY, YQAY) resulted in an increase in the proportion of anti-A β antibody in the CNS. Anti-A β hlgG4 variants showed increased target engagement in the brain compared to WT, as reflected by increased brain A β concentrations (G). Target engagement increased with an increase in brain concentration of the Fc variants (H). Anti-A β hlgG4 Fc variants showed a decrease in circulating endogenous levels of IgG (I). The number of biologically independent animals per group is: for serum and CSF measurements $n = 7$ at Days 0–2, and $n = 5$ at Days 4 and 7; $n = 2$ for all brain measurements. (Statistical significance between Fc variant treated groups and respective WT treated group was evaluated over time by 2-way ANOVA or mixed effect analysis with Tukey or Dunnett's multiple comparisons test using Graphpad Prism 9.5.1; * $p < 0.05$, ** $p < 0.01$, *** $p < 0.001$, **** $p < 0.0001$).

concentration gradient) more rapidly than antibodies that bind poorly to FcRn²⁵ is thus consistent with our findings that engineered antibodies delivered systemically show enhanced brain uptake (also down a concentration gradient).

Along with the brain, improved partitioning was also observed in CSF. This suggests that FcRn plays a role in antibody transport across the blood-CSF barrier in addition to the blood-brain barrier. As higher CSF concentrations track with higher brain concentrations, CSF may serve as a potential surrogate for brain exposure in the clinical setting, although CSF antibody concentration may not directly reflect efflux of antibody from brain to CSF. We also observed increased antibody uptake in some, but not all, peripheral tissues (Suppl. Fig. 7), albeit to an extent less pronounced as compared to the brain. For tissues with tight barriers, such as the brain and the kidney, the contribution of receptor mediated transcytosis pathways is expected to be greater than in tissues with leakier barriers such as the gastrointestinal tract and the lung, where other transport processes such as convection can also play a role. This provides a potential explanation for the apparent

preferential enhancement of uptake of engineered antibodies across the BBB compared to other tissues. The liver is noted to be an exception where despite being a leaky tissue, enhanced uptake was noted. This could potentially be attributed to higher FcRn expression levels in the liver compared to other tissues.

All IgG modifications we tested in vivo increased FcRn binding at pH 6.0 concomitant with the increase at pH 7.4. Since the two cannot be dissociated, it is possible that increased affinity at pH 6.0 also contributes to enhanced transcytosis. Historically, affinity improvements at pH 6.0 alone have only been shown to impact antibody recycling and serum clearance, with no established impact on tissue transcytosis. We submit that it is only when binding at neutral pH is also enabled that the transcytosis feature of FcRn can be realized. A certain threshold of binding affinity at pH 7.4 is likely required to promote transcytosis, and our data suggest this may be $K_D < 1,000$ nM. However, it is possible that transcytosis may be promoted by a combination of increased binding to FcRn at both pH 6.0 and 7.4. While the increased binding at pH 7.4 enables FcRn-mediated uptake into cells,

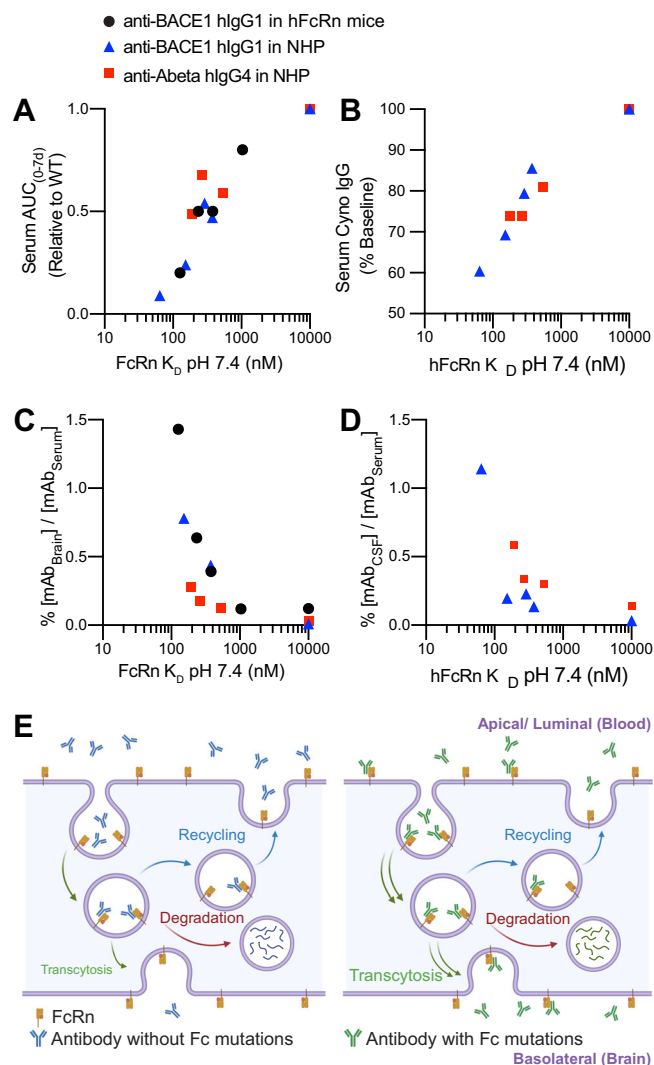


Fig. 6 | Relationship of FcRn affinity at neutral pH with serum clearance, reduction of circulating endogenous IgG levels, and partitioning to the brain and CSF. FcRn affinity at pH 7.4 for the various antibodies tested in hFcRn mouse and NHP studies above is plotted against averages for normalized serum exposure (A), reduction in circulating endogenous IgG (B), fraction of antibody partitioning to brain (C), and fraction of antibody partitioning to CSF (D). Higher affinity antibodies were associated with lower serum exposure and a greater reduction in circulating endogenous IgG, as well as greater partitioning into brain and CSF. Model of cellular trafficking pathways at the BBB impacted by FcRn (E). For WT IgG, most antibodies are recycled back to the apical side (blood), with only a small proportion crossing the BBB by transcytosis (left side). Improved antibody interaction with FcRn at pH 7.4 promotes IgG transcytosis across the BBB (right side). Panel (E) was created in BioRender. Lafrance-Vanasse, J. (2025) <https://BioRender.com/rllvvuy>.

increased binding at pH 6.0 is known to aid lysosomal protection, and the combination may work together to improve transcytosis. In this light, our Fc platform presents something of a paradigm shift from classic Fc engineering approaches, where neutral pH binding to FcRn has generally been viewed as off-limits. Two notable exceptions to this are molecules such as Abdeggs, which are engineered to bind FcRn at neutral pH to clear endogenous IgG, for example for the treatment of autoimmune disease³⁹, and sweeping antibodies, designed to enhance the uptake of antigen-antibody complexes³⁷.

In our experiments, antibodies with enhanced FcRn affinity at neutral pH tended to show faster clearance from serum when dosed intravenously in mice and NHP's. The impact was observed primarily in

the distribution phase, suggesting rapid Fc variant removal from serum. Similar results have been reported in previous studies with antibodies containing some of the same mutations tested here³⁷. Several mechanisms may potentially contribute to the faster serum clearance observed for Fc variants. Increased FcRn degradation by the Fc variant antibodies would theoretically lead to faster clearance of the variants; however, serum albumin levels were not altered in NHPs (Suppl. Fig. 8), suggesting that FcRn expression levels and recycling activity are maintained. Alternatively, increased cellular uptake and transcytosis of the Fc variants in various tissues could directly lead to less endocytosed Fc variants being recycled back to serum, thereby reducing serum exposure. It is also possible that a significant pool of Fc variants remains loosely associated with membrane FcRn and accumulates inside cellular vesicles, such as has been reported for Abdeg molecules³⁹. Such a population of Fc variants could eventually enter a constitutive degradation pathway. Accordingly, productive brain transport may require a balance between achieving sufficient FcRn interaction to promote cellular uptake and transcytosis while avoiding overly tight binding that drives clearance or degradation. The optimal affinity range for enhanced binding to FcRn at pH 7.4 appears to be 150–400 nM in cynomolgus monkey (Table 2).

In cynomolgus monkeys, we saw a sharp decrease in serum antibody exposure after ~7 days for the Fc variants, which may be suggestive of the development of anti-drug antibodies (ADA). FcRn plays a well-established role in antigen presentation by antigen presenting cells (APCs)⁵¹, and tighter FcRn binding may facilitate more efficient presentation. ADA formation has the potential to limit drug exposure and efficacy, and may possibly lead to adverse events. While antibody dosing was well-tolerated in our study, the potential for ADA development and associated safety risks will need to be carefully monitored in future clinical development. Additionally, Fc variants resulted in a reduction of endogenous circulating IgG levels. This effect is reminiscent of FcRn-targeting therapeutics that compete with circulating IgG for FcRn, resulting in a substantial reduction of endogenous IgG, including autoantibodies, for therapeutic benefit³². A potential risk of reduced endogenous IgG levels is lowered immune activity and increased susceptibility to infections. Hypogammaglobulinemia caused by FcRn blockade in humans with approved therapeutics is transient and reversible, and FcRn inhibitors demonstrate an overall acceptable safety profile in multiple autoimmune indications^{53,54}. The reductions in endogenous IgG observed in our studies were reversible, with levels returning to baseline as the FcRn variant IgG's were cleared from the system. Furthermore, as discussed above, we observed no changes in the concentration of serum albumin, which is also recycled by FcRn, suggesting that FcRn intracellular trafficking is not altered (consistent with⁵⁵). Nonetheless, the reduction in endogenous IgG poses a potential risk that should be monitored in further development.

Recent approvals of anti-Amyloid monoclonal antibodies for the treatment of Alzheimer's disease are a milestone in the development of therapeutics for neurodegenerative diseases. The next generation of CNS-directed antibody therapeutics will involve strategies to improve brain uptake. The Fc platform described here represents a promising technology for increasing brain exposure of therapeutic antibodies. Leveraging FcRn for BBB transport can be achieved with modest mutational modification to enhance affinity to a natural Fc receptor, and in an otherwise conventional IgG format that should be easily manufacturable and developable. Furthermore, this platform allows for maintenance of Fab bivalency and Fc effector function, which are desirable features for targets where avidity and/or effector function contribute to mechanism of action. This FcRn platform enhances uptake and partitioning in CSF along with the brain, potentially enabling CSF as a clinically-monitorable surrogate for the brain exposure. Altogether, Fc engineering to promote BBB transport offers a promising new biotherapeutic strategy for improving the

pharmacologic performance of medicines that treat neurodegeneration and other CNS-related disorders.

Methods

Study design

This study was designed to generate and characterize the in vitro and in vivo behavior of antibodies in which the Fc region has been engineered for enhanced binding to FcRn at neutral pH. We generated engineered Fc variants of both mouse and human IgG's, and evaluated their binding affinity to FcRn at both neutral and acidic pH. We characterized the biophysical and functional properties of hIgG1 variants, and tested them in an in vitro cellular transcytosis assay. We next tested several Fc region variants in the context of different Fab's in vivo to assess PK, brain uptake, and brain activity. We used wild-type, PS2APP, or human FcRn-expressing mice, as well as cynomolgus monkeys to understand the translation from mice to non-human primates.

Sample sizes for in vivo studies were determined on the basis of our previous experiences with these animal models and the endpoints being assessed, and kept to a minimal number for ethical reasons. Animals were randomly assigned to groups before experimentation, and researchers were blinded to treatment during data generation and analysis. All analyses were predetermined by experimental protocol. No animal data was excluded. Figure legends contain sample sizes, replicate information, and statistical tests used.

Statistical analysis

Data from animal studies are expressed as individual data points or means \pm SD. For mouse studies, pharmacokinetics non-compartmental analysis was performed using Phoenix WinNonlin 8.2 software (Certara, Radnor PA). Statistical analysis of these studies was performed using GraphPad Prism software (version 9.5.1, Dotmatics, Boston MA). For animal studies, statistical differences between Fc variant treated groups and their respective WT treated groups were evaluated over time by two-way analysis of variance (ANOVA), or mixed effect analysis with Tukey or Dunnett's multiple comparisons test, as indicated in figure legends, unless otherwise indicated. The statistical results including *p*-values for all comparisons that show statistical significance are provided in Suppl. Table 4.

Plasmid construction and antibody production

Antibodies and antibody Fc regions were cloned by standard molecular biology techniques into mammalian expression vectors as previously described⁵⁶. IgGs were expressed as 1 liter transient transfection cultures of Chinese hamster ovary (CHO, Genentech) cells and affinity purified over a GE MAb Select SuRe column (GE Healthcare, Pittsburgh, PA), followed by size exclusion chromatography with a superdex 200 column. All antibody positions are according to the Eu numbering convention. The anti-gD was generated in-house against the glycoprotein D of herpes Simplex Virus, and serves as a negative control as it has no binding target in mammalian models.

Phage display

We adapted a phage display method previously described⁵⁷ to perform a mutational scan of 4 loops of the Fc region, with Fc-displaying phages. Each amino acid of these loops (amino acids 248-259; 284-290; 306-317; 426-438) was randomized with the NNK codon encoding for each 20 amino acids. Each round of panning was done as follows: Murine FcRn-coated plates were blocked with 3% milk, before incubating phage libraries at 37 °C for 2 h in 20 mM MES buffer pH 6.0, 0.05% Tween 20, 3% milk. Plates were washed with 20 mM MES buffer pH6.0, 0.05% Tween 20, 0.3 M NaCl 10–20 times, before eluting phages with PBS pH7.4 at 37 °C for 30 min. The phage libraries were subjected to 3 rounds of panning, before PCR amplification of the Fc

region to submit for Next-Generation Sequencing, using an Illumina MiSeq. The enrichment of mutations was calculated by the following equation: $\log_2(\text{FrqMut}_{\text{sort}}/\text{FrqMut}_{\text{NoSort}})$ where $\text{FrqMut}_{\text{sort}}$ and $\text{FrqMut}_{\text{NoSort}}$ is the frequency of mutated amino acid at a given position in the sorted or unsorted library sample, respectively.

SPR

All SPR experiments were performed at 25 °C on a Biacore T200 instrument (GE Life Sciences, Piscataway, NJ) in HBSP buffer (10 mM Hepes, pH 7.4, 150 mM NaCl, and 0.05% vol/vol Surfactant P20) and MES buffer (100 mM MES pH 6.0, 150 mM NaCl, and 0.05% vol/vol Surfactant P20). Antibodies were captured on an anti-Fab chip and FcRn molecules were injected for 3 min and allowed to dissociate for 3 min at 10 μ l/min. The surface was regenerated between cycles with 10 mM glycine pH 2.1. Affinity constants were obtained by steady state fitting using the Biacore Evaluation Software (GE Life Sciences, Piscataway, NJ). The affinities reported were measured at 25 °C; the affinities at 37 °C were similar (data not shown).

Transcytosis assays

MDCK II cells (CRL-2936, American Type Culture Collection, Manassas, VA) were grown in Dulbecco's modified minimal essential media (Invitrogen, Gaithersburg, MD) containing 10% fetal bovine serum (HyClone Laboratories, Logan, UT) at 37 °C, 5% CO₂. MDCK II cells were stably transfected with human FcRn (*FCGR1* and $\beta_2\text{m}$) and cell lines were expanded from isolated single colonies. All clones were maintained with constant drug selection. For transcytosis assays, $\sim 0.75 \times 10^6$ cells were seeded per each 12 mm diameter, 0.4 μ m pore size filter (CLS3401, Corning Inc., Corning, NY). Transepithelial resistances were recorded daily, the cells fed on day 2 post-plating, and experiments were performed on day 3, when the measured resistances were between 150 and 200 Ωcm^2 . Both surfaces were initially washed with growth media followed by a 24 h incubation at 37 °C, 5% CO₂ with antibody variants. Media from the output solution was collected, and assayed by ELISA as described below. Each antibody was tested in three technical replicates per experiment, and repeated in 2-3 separate experiments.

Animal welfare

In vivo mouse experimental protocols were reviewed and approved by the Genentech Institutional Animal Care and Use Committee. All work was conducted according to NIH guidelines for the humane care and treatment of laboratory animals. Mice were co-housed in a specific-pathogen free (SPF) animal facility with a 14 h light/10 h dark light cycle with ad libitum access to water and food. Cynomolgus monkey studies were conducted at Northern Biomedical Research (Spring Lake, MI) in compliance with the USDA Animal Welfare Act and with approval by local Institutional Animal Care and Use Committees. Monkeys were individually housed in a specific-pathogen free (SPF) animal facility with access to tap water ad libitum, were fed a certified primate diet (PMI Nutritional International Inc.) twice daily, and were given various cage enrichment devices and fruits, vegetables, or dietary enrichment for the duration of the studies.

Wild-type and transgenic mouse models for PK and PD studies

Wild-type female mice ages 6–8 weeks were used for the majority of PK and PD studies. C57B/6 (JAX stock #000664) or SCID (JAX stock #001303) mice were used for mFcRn studies. For mouse studies to model hFcRn, 6–8-week old transgenic Tg32 mice expressing the human FcRn alpha-chain (*FCGR1*) transgene under control of a human promoter and harboring a knockout allele of the mouse FcRn alpha-chain (*Fcgrt*) gene - B6.Cg-*Fcgrt*^{tm1Dcr} Tg(FCGR1)32Dcr/DcrJ (JAX stock #014565) were used^{31,58}. All in vivo β antibody binding studies used 6- to 12-month-old plaque-bearing male and/or female PS2APP mice (in-house colony) on a homozygous C57BL/6 background⁴². PS2APP mice

co-express human APP (hAPP) with the Swedish mutation K670N/M671L and human presenilin 2 with the N141I mutation, driven by Thy1 and PrP promoters, respectively.

Dosing and sample collection for mouse studies

Mice were intravenously injected with the indicated dose of antibody as described. At various times following dosing, blood was collected and either plasma or serum isolated for measurement of antibody concentration. For plasma collection, whole blood was collected in EDTA microtainer tubes (BD Diagnostics, Franklin Lake, NJ) prior to perfusion, centrifuged at 5,000 \times g for 15 min and the supernatant was isolated for measuring plasma antibody concentrations. For serum collection, whole blood was collected in serum separator micro-container tubes (BD Diagnostics, Franklin Lake, NJ), allowed to clot for at least 30 min, and spun down at 5,000 \times g for 90 s. The supernatant was isolated for serum antibody measurements. At the indicated times, mice were euthanized by exsanguination through cardiac perfusion with D-PBS under sedation, and brains were collected for measurement of antibody concentration and/or A β . For brain antibody concentration measurements, a hemi-brain from each mouse was homogenized in 1% NP-40 (492016, Sigma Aldrich, St. Louis, MO) in PBS containing Roche Complete Mini EDTA-free protease inhibitor cocktail tablets (11836170001, Sigma Aldrich, St. Louis, MO). Homogenized brain samples were rotated at 4 °C for 1 h before centrifugation at 14,000 rpm for 20 min. The supernatant was isolated for brain antibody measurement. For A β ₁₋₄₀ measurements, hemi-brains were homogenized in 5 M guanidine hydrochloride buffer and samples rotated for 3 h at room temperature prior to dilution (1:10) in 0.25% casein, 5 mM EDTA (pH 8.0) in PBS containing freshly added aprotinin (20 mg/mL) and leupeptin (10 mg/mL). Diluted homogenates were centrifuged at 14,000 rpm for 20 min and supernatants were isolated for A β ₁₋₄₀ measurement.

Measuring antibody concentrations in mouse plasma, serum, and brain (pharmacokinetics)

Total antibody concentrations in mouse plasma, serum, or brain homogenate were measured with a generic human IgG ELISA. Nunc 384-well MaxiSorp immunoplates (464718, Thermo Fisher Scientific, Waltham, MA) were coated with 0.5 μ g/mL F(ab')₂ fragment of donkey anti-human IgG and Fc fragment-specific polyclonal antibody (709-006-098, Jackson ImmunoResearch, Westgrove PA) overnight at 4 °C. Plates were blocked with PBS and 0.5% bovine serum albumin (BSA) for 1 h at 25 °C. Each antibody (control IgG or modified Fc) was used as a standard to quantify respective antibody concentrations. Plates were washed with PBS and 0.05% Tween 20 using a microplate washer (Bio-Tek Instruments Inc.), and standards and samples diluted in PBS containing 0.5% BSA, 0.35 M NaCl, 0.25% CHAPS, 5 mM EDTA, 0.05% Tween 20, and 15 ppm (parts per million) Proclin were added for 2 h at 25 °C. Bound antibody was detected with HRP-conjugated F(ab')₂ goat anti-human IgG and Fc-specific polyclonal antibody (109-036-098, Jackson ImmunoResearch, Westgrove PA), 1:5000, and developed with KPL TMB (5120-0077, SeraCare, Milford, MA) for 20 min followed by 1 M Phosphoric acid to stop the reaction, and absorbance (A) was measured at 450 nm on a Multiskan Ascent reader (Thermo Fisher Scientific, Waltham, MA). Concentrations were determined from the standard curve with a four-parameter nonlinear regression program.

PD assays for mouse brain

A β ₁₋₄₀ concentrations in mouse brain samples were measured using an ELISA similar to methods described above for PK analysis. Briefly, 1 μ g/mL rabbit polyclonal antibody specific for A β ₁₋₄₀ (Genentech) was coated onto plates, and biotinylated anti-mouse A β monoclonal antibody M3.2 (SIG-39155, BioLegend, San Diego, CA) was used for detection. The assay had a lower limit of quantification values of 1.96 pg/mL in plasma and 39.1 pg/g in brain.

Anti-A β in vivo dosing studies

Transgenic PS2APP mice were randomized into treatment groups and received a single intravenous (IV) dose of either anti-A β hlgG4 or anti-A β -YTE hlgG4 at 20 mg/kg diluted in platform buffer (20 mM histidine, 240 mM sucrose; pH 5.5, 0.02% Tween 20) and injected at a volume of 5 mL/kg. Five days after dosing, the animals were euthanized as described above, and terminal plasma was collected via cardiac puncture prior to perfusion with phosphate-buffered saline (PBS). The cerebellum was dissected, weighed, and stored at -80 °C for later processing to measure antibody PK. The right hemibrain was drop-fixed in 4% paraformaldehyde for 48 h and then transferred to 30% sucrose in PBS. Free-floating sagittal cryosections (35 μ m) of mouse brain were washed in PBS and then PBS-Triton X100 (PBST, 0.1%) and then blocked in PBST (0.3%) with 5% bovine serum albumin (BSA) and incubated overnight with primary antibodies diluted in 1% BSA in PBST (0.3%) at 4 °C. Goat anti-human IgG-Alexa647 (A21445, 1:100-1:500; Thermo Fisher Scientific, Waltham, MA) was used to localize the administered human antibody. Plaques were detected using the A β fluorescent marker methoxy-X04 at 10 μ M in 40% ethanol in PBS (4920, R&D Systems, Minneapolis, MN).

Fluorescent microscopy

Whole slide images are captured at 20 \times using a Panoramic 250 (3D Histech, Hungary) equipped with PCO.edge camera (Excelitis, Kelheim, Germany), Lumencor Spectra X (Beaverton, OR), and Semrock filters (Rochester, NY) optimized for 4'-diamidino-2-phenylindole, dihydrochloride (DAPI), tetramethylrhodamine isothiocyanate (TRITC), and cyanine 5 (Cy5) fluorophores. Ideal exposure for each channel is determined based on samples with the brightest intensity and is set for the whole set of slides to run as a batch. Images were also captured at 20 \times using a Leica DM5500B light microscope using Leica Application Suite Advanced Fluorescence software (LAS AF4.0). Quantification of mossy fiber staining was performed by measuring integrated density from two to four sections per animal using ImageJ (NIH).

Dosing and sample collection for cynomolgus monkey studies

Anti-BACE1 hlgG1 studies. For both studies, four male cynomolgus monkeys aged 3–5 years were used per experimental group. In the first study, anti-BACE1 hlgG1 wild-type antibody, and anti-BACE1 hlgG1 antibodies with modified Fcs (anti-BACE1-YQAY, YEY, YPY) were administered at 50 mg/kg via an intravenous bolus injection into the saphenous vein at day 0. CSF and blood samples were collected at various time points from 7 days before dosing up to 29 days post dose. Samples were collected at the same time of the day. In the second study, anti-BACE1 hlgG1 wild-type antibody, and anti-BACE1 hlgG1 antibodies with modified Fcs (anti-BACE1-YQAY, YY) were administered at 50 mg/kg via an intravenous bolus injection into the saphenous vein. CSF and blood samples were collected at various time points from 7 days before dosing up to 7 days after dosing. At 2 and 7 days post-dose, two animals each were euthanized. Animals were sedated with ketamine, maintained on an isoflurane/oxygen mixture, and provided with an IV bolus of heparin sodium. The animals were then perfused via the left cardiac ventricle with chilled 0.001% sodium nitrite in saline. Brain and several peripheral tissues were harvested after full body perfusion. Brain regions (frontal cortex, temporal cortex, hippocampus) were sub-dissected and immediately frozen.

Anti-A β hlgG4 study. Four male cynomolgus monkeys aged 3–5 years were used per experimental group. Anti-A β hlgG4 wild-type antibody, and anti-A β hlgG4 antibodies with modified Fcs (anti-A β -YQAY, YEY, YY) were administered at 50 mg/kg via an intravenous bolus injection into the saphenous vein at day 0. CSF and blood samples were collected at various time points from 7 days before dosing up to 7 days

post dose. Samples were collected at the same time of the day. At 2 and 7 days post-dose, two animals each were euthanized as described above, and brains and several peripheral tissues were harvested after full body perfusion. Brain regions were sub-dissected and immediately frozen.

Various brain regions and peripheral tissues were homogenized in 1% NP-40 (492016, Sigma Aldrich, St. Louis, MO) in PBS containing Roche Complete Mini EDTA-free protease inhibitor cocktail tablets (11836170001, Sigma Aldrich, St. Louis, MO). Homogenized brain samples were rotated at 4 °C for 1 h before spinning at 14,000 rpm for 20 min. The supernatant was isolated for brain PK and PD. Brain data from frontal cortex, temporal cortex and hippocampus were combined and averaged to present the average value per animal across these brain regions.

Measuring antibody concentrations in cynomolgus monkey samples

For anti-BACE1 serum samples, total antibody concentrations were measured by mixing samples with SILuMAB (#MSQC3, Sigma Aldrich, St. Louis, MO) internal standard (a stable isotopically labeled IgG1 monoclonal antibody) and using an LC-MS/MS method with affinity capture using Protein A followed by Rapigest denaturation, reduction, alkylation and tryptic digestion. The digested samples were injected into the Eksigent microLC 200 UPLC system (AB SCIEX, Framingham, MA) coupled online to an AB Sciex QTrap 5500 Mass Spectrometer. Chromatographic separation was performed on Phenomenex Luna C18 (Phenomenex, Torrance, CA), 50 × 1 mm, 3 μm, 100 Å column using a gradient of mobile phase A (0.1% formic acid in water) and mobile phase B (0.1% formic acid in acetonitrile) at a flow rate of 50 μL min⁻¹. A 5 min gradient from 5% B (0.5 min) to 45% B (5.5 min) to 95% B (6.5 min) was used, followed by wash and re-equilibration. The signature peptide TTPVLDSDGSFFLYSK from the Fc region was selected as the surrogate analyte for the quantification of the total antibody concentration.

For anti-Aβ detection in cyno serum, as well as all CSF and brain samples, total human antibody concentrations were measured using a generic total human IgG ELISA. Nunc MaxiSorp 384-well plates (464718, Thermo Fisher Scientific, Waltham, MA) were coated with 0.5 μg/mL monkey adsorbed sheep anti-Human IgG (AU003.M, Binding Site, San Diego, CA) diluted in 0.05 M carbonate/bicarbonate buffer pH 9.6 and incubated overnight at 4 °C. The plates were washed 3 times with wash buffer (0.05% Tween-20 in PBS buffer, pH 7.4) and treated with block buffer (PBS/0.5% BSA/15 ppm Proclin, pH 7.4) for 1 to 2 h at room temperature (RT). The plates were washed 3 times with wash buffer and then samples diluted in sample diluent (PBS/0.5% BSA/0.05% Tween 20/5 mM EDTA/0.25% CHAPS/0.35 M NaCl/15 ppm Proclin, pH 7.4) were added to the wells and incubated for 2 h at RT with gentle agitation. After washing the plates 6 times with wash buffer, a detection antibody, horseradish peroxidase (HRP) conjugated –monkey adsorbed goat anti-Human IgG (A80-319P-12, Bethyl Laboratories, Montgomery, TX), diluted to 100 ng/mL in assay buffer (PBS/0.5% BSA/15 ppm Proclin/0.05% Tween 20, pH 7.4) was added to the wells and incubated on a shaker for 1 h at RT. The plates were washed 6 times with wash buffer and developed using KPL TMB peroxidase substrate (5120-0077, SeraCare, Milford, MA) for 20 min followed by 1 M Phosphoric acid to stop the reaction. Absorbance was measured at 450 nm against a reference wavelength of 620 nm. The concentration of the samples was extrapolated from a 4-parameter fit of the standard curve.

Total cyno IgG concentrations in cyno serum samples were measured using an ELISA similar to methods described above for PK analysis. Briefly, 2 μg/mL goat anti-monkey IgG antibody (A140-202A, Bethyl Laboratories, Montgomery, TX) was coated onto plates, and biotinylated goat anti-monkey IgG antibody (A140-202A, Bethyl Laboratories, Montgomery, TX) was used for detection. The plates were washed 6 times with wash buffer and developed using TMB

peroxidase substrate (TMBE-1000, Moss Inc., Pasadena, MD) for 20 min followed by 1 M Phosphoric acid to stop the reaction.

Pharmacodynamics assays

sAPPβ/α ratio. CSF and brain concentrations of sAPPα and sAPPβ were determined with the MSD 96-well MULTI-SPOT sAPPα/sAPPβ ECL assay (Meso Scale Discovery, Rockland, MD). Plates were coated with monoclonal antibodies specific for capture of sAPPα and APPβ. Both analytes were detected with an antibody directed against the N-terminus of APP. CSF was thawed on ice and then diluted 1:10 into 1% BSA in TBS–Tween 20. The assay had LLOQ values of 0.05 and 0.03 ng/ml for sAPPα and sAPPβ, respectively.

Aβ₁₋₄₂ assay. The concentration of Aβ₁₋₄₂ in cynomolgus monkey brain was determined using an ELISA similar to methods described above for PK analysis. Briefly, 3 μg/mL rabbit polyclonal capture antibody specific for the C terminus of Aβ₄₂ (700254, Thermo Fisher Scientific, Waltham, MA) was coated onto plates, and biotinylated anti-Aβ monoclonal antibody 6E10

(803007, BioLegend, San Diego, CA) was used for detection. The assay had a limit of quantification values of 23.44 pg/mL in brain lysate.

Reporting summary

Further information on research design is available in the Nature Portfolio Reporting Summary linked to this article.

Data availability

All data are included in the Supplementary Information or available from the authors, as are unique research reagents used in this Article. The raw numbers for charts and graphs are available in the Source Data file whenever possible. Source data are provided with this paper.

References

1. Jefferies, W. A. et al. Transferrin receptor on endothelium of brain capillaries. *Nature* **312**, 162–163 (1984).
2. Fishman, J. B., Rubin, J. B., Handrahan, J. V., Connor, J. R. & Fine, R. E. Receptor-mediated transcytosis of transferrin across the blood-brain barrier. *J. Neurosci. Res.* **18**, 299–304 (1987).
3. Pardridge, W. M., Buciak, J. L. & Friden, P. M. Selective transport of an anti-transferrin receptor antibody through the blood-brain barrier in vivo. *J. Pharm. Exp. Ther.* **259**, 66–70 (1991).
4. Yu, Y. J. et al. Boosting brain uptake of a therapeutic antibody by reducing its affinity for a transcytosis target. *Sci. Transl. Med.* **3**, 84ra44 (2011).
5. Niewoehner, J. et al. Increased brain penetration and potency of a therapeutic antibody using a monovalent molecular shuttle. *Neuron* **81**, 49–60 (2014).
6. Kariolis, M. S. et al. Brain delivery of therapeutic proteins using an Fc fragment blood-brain barrier transport vehicle in mice and monkeys. *Sci. Transl. Med.* **12**, eaay1359 (2020).
7. Yu, Y. J. et al. Therapeutic bispecific antibodies cross the blood-brain barrier in nonhuman primates. *Sci. Transl. Med.* **6**, 261ra154 (2014).
8. Couch, J. A. et al. Addressing safety liabilities of TFR bispecific antibodies that cross the blood-brain barrier. *Sci. Transl. Med.* **5**, 183ra57 (2013).
9. Weber, F. et al. Brain shuttle antibody for alzheimer's disease with attenuated peripheral effector function due to an inverted binding mode. *Cell Rep.* **22**, 149–162 (2018).
10. Lo, M. et al. Effector-attenuating substitutions that maintain antibody stability and reduce toxicity in mice. *J. Biol. Chem.* **292**, 3900–3908 (2017).
11. Okuyama, T. et al. A phase 2/3 trial of pabinafusp alfa, IDS fused with anti-human transferrin receptor antibody, targeting neurodegeneration in MPS-II. *Mol. Ther.* **29**, 671–679 (2021).

12. Giugliani, R. et al. Enzyme replacement therapy with pabinafusp alfa for neuronopathic mucopolysaccharidosis ii: an integrated analysis of preclinical and clinical data. *Int. J. Mol. Sci.* **22**, 10938 (2021).
13. Zuchero, Y. J. Y. et al. Discovery of novel blood-brain barrier targets to enhance brain uptake of therapeutic antibodies. *Neuron* **89**, 70–82 (2016).
14. Boado, R. J., Lu, J. Z., Hui, E. K.-W., Lin, H. & Pardridge, W. M. Bi-functional IgG-lysosomal enzyme fusion proteins for brain drug delivery. *Sci. Rep.* **9**, 18632 (2019).
15. Sheff, J. et al. Defining the epitope of a blood–brain barrier crossing single domain antibody specific for the type 1 insulin-like growth factor receptor. *Sci. Rep.* **11**, 4284 (2021).
16. Shin, J.-W. et al. Grabody B, an IGF1 receptor-based shuttle, mediates efficient delivery of biologics across the blood-brain barrier. *Cell Rep. Methods* **2**, 100338 (2022).
17. Chew, K. S. et al. CD98hc is a target for brain delivery of biotherapeutics. *Nat. Commun.* **14**, 5053 (2023).
18. Schlachetzki, F., Zhu, C. & Pardridge, W. M. Expression of the neonatal Fc receptor (FcRn) at the blood–brain barrier. *J. Neurochem* **81**, 203–206 (2002).
19. Latvala, S., Jacobsen, B., Otteneder, M. B., Herrmann, A. & Kronenberg, S. Distribution of FcRn across species and tissues. *J. Histochem. Cytochem.* **65**, 321–333 (2017).
20. Ghetie, V. et al. Abnormally short serum half-lives of IgG in β 2-microglobulin-deficient mice. *Eur. J. Immunol.* **26**, 690–696 (1996).
21. Challa, D. K., Velmurugan, R., Ober, R. J. & Ward, E. S. Fc Receptors. *Curr. Top. Microbiol.* **382**, 249–272 (2014).
22. Firan, M. et al. The MHC class I-related receptor, FcRn, plays an essential role in the maternofetal transfer of γ -globulin in humans. *Int. Immunol.* **13**, 993–1002 (2001).
23. Wheeler, T. T., Hodgkinson, A. J., Prosser, C. G. & Davis, S. R. Immune components of colostrum and milk—a historical perspective. *J. Mammary Gland Biol.* **12**, 237–247 (2007).
24. Abuqayyas, L. & Balhasar, J. P. Investigation of the Role of Fc γ R and FcRn in mAb distribution to the brain. *Mol. Pharm.* **10**, 1505–1513 (2013).
25. Cooper, P. R. et al. Efflux of monoclonal antibodies from rat brain by neonatal Fc receptor, FcRn. *Brain Res.* **1534**, 13–21 (2013).
26. Kuo, T. T. & Aveson, V. G. Neonatal Fc receptor and IgG-based therapeutics. *mAbs* **3**, 422–430 (2011).
27. Ghetie, V. & Ward, E. S. Transcytosis and catabolism of antibody. *Immunol. Res.* **25**, 97–113 (2002).
28. Hinton, P. R. et al. Engineered human IgG antibodies with longer serum half-lives in primates. *J. Biol. Chem.* **279**, 6213–6216 (2004).
29. Dall’Acqua, W. F., Kiener, P. A. & Wu, H. Properties of human IgG1s engineered for enhanced binding to the neonatal fc receptor (FcRn). *J. Biol. Chem.* **281**, 23514–23524 (2006).
30. Hinton, P. R. et al. An engineered human IgG1 antibody with longer serum half-life. *J. Immunol.* **176**, 346–356 (2006).
31. Petkova, S. B. et al. Enhanced half-life of genetically engineered human IgG1 antibodies in a humanized FcRn mouse model: potential application in humorally mediated autoimmune disease. *Int. Immunol.* **18**, 1759–1769 (2006).
32. Datta-Mannan, A., Witcher, D. R., Tang, Y., Watkins, J. & Wroblewski, V. J. Monoclonal antibody clearance. Impact of modulating the interaction of IgG with the neonatal Fc receptor. *J. Biol. Chem.* **282**, 1709–1717 (2007).
33. Yeung, Y. A. et al. Engineering human IgG1 affinity to human neonatal fc receptor: impact of affinity improvement on pharmacokinetics in primates. *J. Immunol.* **182**, 7663–7671 (2009).
34. Zalevsky, J. et al. Enhanced antibody half-life improves in vivo activity. *Nat. Biotechnol.* **28**, 157–159 (2010).
35. Robbie, G. J. et al. A novel investigational Fc-modified humanized monoclonal antibody, motavizumab-YTE, has an extended half-life in healthy adults. *Antimicrob. Agents Ch.* **57**, 6147–6153 (2013).
36. Gaudinski, M. R. et al. Safety and pharmacokinetics of the Fc-modified HIV-1 human monoclonal antibody VRC01LS: a phase 1 open-label clinical trial in healthy adults. *Plos Med.* **15**, e1002493 (2018).
37. Igawa, T. et al. Engineered monoclonal antibody with novel antigen-sweeping activity in vivo. *Plos One* **8**, e63236 (2013).
38. Acqua, W. F. D. et al. Increasing the affinity of a human IgG1 for the neonatal fc receptor: biological consequences. *J. Immunol.* **169**, 5171–5180 (2002).
39. Vaccaro, C., Zhou, J., Ober, R. J. & Ward, E. S. Engineering the Fc region of immunoglobulin G to modulate in vivo antibody levels. *Nat. Biotechnol.* **23**, 1283–1288 (2005).
40. Borrok, M. J. et al. pH-dependent Binding engineering reveals an FcRn affinity threshold that governs IgG recycling. *J. Biol. Chem.* **290**, 4282–4290 (2015).
41. Tam, S. J. et al. Death receptors DR6 and TROY regulate brain vascular development. *Dev. Cell* **22**, 403–417 (2012).
42. Ozmen, L., Albientz, A., Czech, C. & Jacobsen, H. Expression of transgenic APP mRNA is the key determinant for beta-amyloid deposition in PS2APP transgenic mice. *Neurodegener. Dis.* **6**, 29–36 (2008).
43. Meilandt, W. J. et al. Characterization of the selective in vitro and in vivo binding properties of crenezumab to oligomeric A β . *Alzheimer’s Res. Ther.* **11**, 97 (2019).
44. Martin, W. L., West, A. P., Gan, L. & Bjorkman, P. J. Crystal structure at 2.8 Å of an FcRn/heterodimeric Fc complex mechanism of pH-dependent binding. *Mol. Cell* **7**, 867–877 (2001).
45. Gadkar, K. et al. Mathematical PKPD and safety model of bispecific TfR/BACE1 antibodies for the optimization of antibody uptake in brain. *Eur. J. Pharm. Biopharm.* **101**, 53–61 (2016).
46. Igawa, T., Haraya, K. & Hattori, K. Sweeping antibody as a novel therapeutic antibody modality capable of eliminating soluble antigens from circulation. *Immunol. Rev.* **270**, 132–151 (2016).
47. Chung, S. et al. An in vitro FcRn-dependent transcytosis assay as a screening tool for predictive assessment of nonspecific clearance of antibody therapeutics in humans. *Mabs* **11**, 942–955 (2019).
48. Yamada, K. et al. A immunotherapy: intracerebral sequestration of a by an anti-a monoclonal antibody 266 with high affinity to soluble A. *J. Neurosci.* **29**, 11393–11398 (2009).
49. Pardridge, W. M. CSF, blood-brain barrier, and brain drug delivery. *Expert Opin. Drug Del.* **13**, 963–975 (2016).
50. Tien, J. et al. Modifying antibody-FcRn interactions to increase the transport of antibodies through the blood-brain barrier. *mAbs* **15**, 2229098 (2023).
51. Baker, K., Rath, T., Pyzik, M. & Blumberg, R. S. The role of FcRn in antigen presentation. *Front Immunol.* **5**, 408 (2014).
52. Gable, K. L. & Guptill, J. T. Antagonism of the neonatal fc receptor as an emerging treatment for Myasthenia Gravis. *Front Immunol.* **10**, 3052 (2020).
53. Peter, H.-H. et al. Targeting FcRn for immunomodulation: benefits, risks, and practical considerations. *J. Allergy Clin. Immun.* **146**, 479–491.e5 (2020).
54. Li, J. et al. The efficacy and safety of FcRn inhibitors in patients with myasthenia gravis: a systematic review and meta-analysis. *J. Neurol.* **271**, 2298–2308 (2024).
55. Patel, D. A. et al. Neonatal Fc receptor blockade by Fc engineering ameliorates arthritis in a murine model. *J. Immunol.* **187**, 1015–1022 (2011).
56. Eaton, D. L. et al. Construction and characterization of an active factor VIII variant lacking the central one-third of the molecule. *Biochem. US* **25**, 8343–8347 (1986).

57. Koenig, P. et al. Deep sequencing-guided design of a high affinity dual specificity antibody to target two angiogenic factors in neovascular age-related macular degeneration. *J. Biol. Chem.* **290**, 21773–21786 (2015).
58. Roopenian, D. C., Christianson, G. J. & Sproule, T. J. Mouse models for drug discovery, methods and protocols. *Methods Mol. Biol. Clifton N. J.* **602**, 93–104 (2006).

Acknowledgements

We thank Paul Carter, Jesse Hanson and Baris Bingol for providing input on this manuscript. We thank the gRED Nonclinical Operations In Vivo Studies (IVS) group for assistance in executing mouse experiments. Some figures were created with BioRender.com. The preclinical studies were funded by Genentech Inc., South San Francisco, CA.

Author contributions

S.S.S., D.B.Y., W.J.M., S.R.C., S.C., G.A.L., J.A.E. and J.K.A. designed the research. J.L.-V., Y.Y., W.J.M., M.K.W.-S., V.N., V.L., B.C., M.K. and P.C. performed experiments. S.S.S., Y.Y., D.B.Y., W.J.M., M.K.W.-S., H.C., S.R.C., V.N., V.L., B.C., M.K., P.C., S.S., D.L., S.C., G.A.L. J.A.E. and J.K.A. analyzed data. J.L.-V., S.S.S., G.A.L. and J.K.A. wrote the manuscript.

Competing interests

J.L.-V., S.S.S., Y.Y., D.B.Y., W.J.M., M.K.W.-S., H.C., S.R.C., V.N., V.L., B.C., M.K., P.C., S.S., D.L., S.C., G.A.L., J.A.E., J.K.A. are or were employees of Genentech Inc., a member of the Roche Group, and may hold Roche stock or related interests. S.S.S., Y.Y., S.C., G.A.L., J.A.E., J.K.A. are inventors on WO/2020/132230 and U.S. Pub. No. US20220033520A1 entitled “Modified antibody fcs and methods of use”.

Additional information

Supplementary information The online version contains supplementary material available at <https://doi.org/10.1038/s41467-025-59447-1>.

Correspondence and requests for materials should be addressed to Jasvinder K. Atwal.

Peer review information *Nature Communications* thanks Reina Benda-yan, Martin Lauritzen and Jason Tien for their contribution to the peer review of this work. A peer review file is available.

Reprints and permissions information is available at <http://www.nature.com/reprints>

Publisher's note Springer Nature remains neutral with regard to jurisdictional claims in published maps and institutional affiliations.

Open Access This article is licensed under a Creative Commons Attribution-NonCommercial-NoDerivatives 4.0 International License, which permits any non-commercial use, sharing, distribution and reproduction in any medium or format, as long as you give appropriate credit to the original author(s) and the source, provide a link to the Creative Commons licence, and indicate if you modified the licensed material. You do not have permission under this licence to share adapted material derived from this article or parts of it. The images or other third party material in this article are included in the article's Creative Commons licence, unless indicated otherwise in a credit line to the material. If material is not included in the article's Creative Commons licence and your intended use is not permitted by statutory regulation or exceeds the permitted use, you will need to obtain permission directly from the copyright holder. To view a copy of this licence, visit <http://creativecommons.org/licenses/by-nc-nd/4.0/>.

© The Author(s) 2025